Dear editor, dear reviewers,

We thank the two reviewers for their second round of comments, and the responses to these comments are given below along with a marked-up version of the text. Two changes are notable: first, in responding to Reviewer 1's first major comment, we have implemented the Bayesian Information Criterion to select a coherent number of change points. We also eliminate the use of a constant probability threshold, which Reviewer 1 found to be a design flaw, in favor of selecting the $n-2$ (or fewer) contiguous probability peaks with greatest integrated probability (and apart from some small regions, there are generally only $n-2$ or less visible peaks).

In addition, we have updated our results to include the d18O stack of Buizert et al. (2018), mentioned by one of the reviewers, which was made with more up-to-date volcanic synchronizations between the four East Antarctic cores and the WAIS Divide cores, using Sulfate instead of ECM data, is more reliable, and presents less chronological uncertainty.

These changes, importantly, do not significantly change the results of our paper.

Finally, we thank the editor as well for his detailed comments, which we have also taken into account.

All the best, on behalf of all co-authors,

Jai Chowdhry Beeman

Reviewer 1

The authors have addressed several of my concerns regarding the methodology and improved their manuscript significantly. However, there remain a number of points in the methodology that in my opinion require further consideration:

1. I disagree with the authors' statement that they can investigate more change-points than the number defined in the model (which is 6+2). Each realization of the MCMC fits the data with n change-points. Hence, the PDF is also only true for the defined n. In their reply to my previous comment, the authors state that they generate one continuous PDF for the likelihood of a given x being a change-point, and that this PDF can have multiple (more than n) peaks. It is of course true, that there can be more than n peaks in the PDF, but some of them will be modes of the same change-point and thus, mutually exclusive. It would thus be more informative to generate one PDF per change-point. The way MCMC works, I am surprised that this posterior distribution for each change-point is not standard output of the method. This would affect the error estimates on the change-points and thus, the inferred delays. Furthermore, it would affect the significance test. Currently, the absolute probability threshold does not measure significance but precision. We can easily imagine how few iterations placing a change-point in the same location create a high and narrow peak in the PDF. On the other hand, many iterations placing a change-point into a slightly more variable location will result in a wider and thus, lower peak in the PDF. The cumulative probability is however higher in the latter example. Eventually, it is not a question of how many significant change-points there are: By defining n change-points, the answer is n. The question would then be whether a model with more/less change-points leads to a significantly improved fit to the data. Ideally, I would like the authors to address this and show posterior distribution per change-point. However, given the tests with more (SI) and less (SI of previous version of the manuscript) change-points I can also see how treating the change-points separately would probably not change the results drastically. Thus, I would appreciate if the authors could include both figures (more and less change-points, the latter also updated with the AR-model of this version of the manuscript) in the supplementary materials and add a short section in the main text, where they discuss the differences with respect to change-points and the resulting delays. I would appreciate if the authors could be more explicit/quantitative in their discussion of the differences than in this version of the manuscript (P8, L5-6: "probability distributions with 8 and 10 points are rather similar.") since the choice of number of change-points is ultimately arbitrary and represents an uncertainty in the method.

— First, let us address the idea of treating the change points individually. A few examples can illustrate how this approach, while it would be practical for the method, is not correct.

Unlike previously developed change point fitting methods (i.e. Parrenin et al., 2013), we do not specify an initial position for the change points. Instead, we randomly initialize multiple walkers over a distribution uniform in time. The randomized initialization helps us reduce subjectivity in the method, and the use of multile walkers helps prevent the simulation from becoming stuck in local minima. As the MCMC simulation proceeds, the walkers converge towards the posterior distribution.

However, importantly, this does not mean that they converge toward one "best fit" solution. Rather, multiple approximate solution should be accepted proportionally to their probability.

Consider two fits accepted during the MCMC simulation with a gradual change. It is probable to accept a change point during this gradual change, and probable to not accept one at all. If in the first case the 5th point was fit in the gradual change and the 6th point at the next change point, in the second case the 5th point will be fit at the next change point, and the 6th afterward.

If, for example, the gradual change occurs at 10 ky BP and the next change at 5 ky BP, it is not reasonable to treat these as modes of the same change point, even though they are both fit by the 5th point. Similarly, it is not reasonable to treat the two points fitted at 5 ky BP as mutually exclusive, simply because one is fitted by the second change point and one the third. We cannot neglect the physical reality of there being only one change here for statistical convenience.

The reviewer's statement "eventually, it is not a question of how many significant change-points there are: By defining n change-points, the answer is n" has considerable value. Indeed, we can take the $n-2$ (or fewer) contiguous regions of highest cumulative probability for a given number of points, which provides a consistent solution. Unlike the maximum probability threshold used in the previous iteration of this manuscript, this allows us to treat contiguous regions of high cumulative probability consistently, whether the maximum histogram bin value is high or low. In the case that there are less than n contiguous regions of cumulative probability, we can assume that there are indeed less than n significant change points. The marked tests of various numbers of points to fit the temperature stack are an example of this.

Selecting n is then the next challenge. We do this by applying the Bayesian Information Criterion (BIC) to our two series. The normalized, summed BIC for the linear models of both series suggests that n=8 is the most parsimonious solution (Supplementary Figure 2, shown below as well). However, because the BIC is merely a criterion, we still include fits with 5,6,7,8 and 9 points in the supplement. We also provide timings and lead-lag estimates for n=7 points in the supplementary spreadsheet.

The BIC is treated in detail in section 2.4 of the manuscript, and in supplementary Figure 7.

2. The AR-model should also be applied to the filtered data. In the manuscript the authors state (P 10, L11-12): "In the two filtered series, the sub-millenial scale AR(1) noise present in the original series should be essentially removed. As such, fitting change points to these two series, assuming the residuals to be uncorrelated, provides a second form of verification of the appropriateness of the covariance matrix we use to fit the raw data." This is not true. Savitsky-Golay filters are smoothing filters that do not remove, but introduce autocorrelation. It is obvious that data filtered with a 500yr cutoff but supplied at 200yr resolution cannot be white noise. Furthermore, the method itself estimates autocorrelation (equation 2 and 3) and thus, if "a" in eq. 2 and 3 was indeed zero, then the method should detect it, set "a" to zero and hence, treat it as white noise automatically. Please, redo the analysis and figure 4 accordingly.

Accepted. This figure is redone (Figure 4).

3. The authors point out correctly, that the PDFs of the change-points are multimodal and skewed and should hence not be reported as $\mu \pm \sigma$. Looking at figure 6 I believe the same is true for the lead/lag PDFs. Please, throughout the manuscript, provide the most likely values (probability peak) and the 68.2/95.4% probability intervals.

Accepted. Sigmas are changed to 68/95% confidence intervals in the abstract, section 3.2, section 3.3, the new table 1, and in the conclusions.

4. I apologize for not commenting on this earlier: Could you rearrange the figures so that the time-series and the histograms do not overlap with each other, but are connected with X-gridlines? As it is now, some features discussed in the manuscript are impossible to see in the figures.

Accepted. Figures 3 and 4 are revised so that the series and histograms do not overlap.

Specific Comments:

P1, L7: Delete "abrupt". The method makes no estimate of the abruptness of changes.

Accepted

P1, L11: replace "nearly synchronously" with a more precise "within xx years [68.2% probability]" – the uncertainty is quite big for this change.

Accepted (as done in general.)

P1, L11: "250 years": Figure 6 reads -188±154? Please correct (also according to main comment 3)

Accepted

P1, L12: "after the ACR onset in the temperature record": I think one of the interesting results of this paper is, that this change point is actually only present in East Antarctica (EDC and TD), which could be worthwhile mentioning in the abstract?

This point may be present in WD as well, though it occurs slightly later. It is worth noting that the probability of this change point is lower in the new stack. This observation is perhaps too complex to include clearly in the abstract.

P2, L3: enter spaces before the two en dash uses.

Accepted

P4, L23 and P11, L. 24: Bintanja et al. 2013 is cited as a reference for the correction of water isotope records for source isotopic variations. Is this the correct reference? They do not study isotopes, and focus on the last 30 years? Please check.

Bintanja et al. (2015) is the correct citation, though this is now removed because of the use of the Buizert et al. (2018) stack. The replacement of the stack does not significantly change the results.

Page 5, figure caption 2: "ratio of the age difference". I still don't entirely understand this formulation. Do you mean the ratio of the age difference between neighbouring tie-points on WDC2014 and the same tie-points on EDC (on AICC12?). I.e., if the ratio is 1.01, then the duration between tie-points differs by 1% between the two independent timescales? Please clarify.

The stack is now replaced, and uncertainty calculated as in Buizert et al. (2018).

Page 5, figure caption 2: The 20% uncertainty is assumed to be 1 sigma? If so please change to: "... which is determined as 20% (1σ) of the distance to the nearest tie point, ..."

The stack is replaced, and uncertainty calculated as in Buizert et al. (2018).

P6, L6: "... and can improve the balance of precision and accuracy of the fits." What do you mean? Delete?

Deleted

P6, L7: "related with" replace "related to"

Accepted

P6, L9: "first source of uncertainty" replace with "measurement uncertainty"

Accepted

P6, L15-17: "These challenges can be circumvented…" That would only be true if we knew that the resolution was lower than the decorrelation time. Is this the case? Looking at figure 4 in Parrenin et al. also there the residuals are autocorrelated. Delete?

Accepted

P7, L32-33: replace "confirm" with "test" and "is accurate" with "cannot be rejected".

Accepted

P7, L33: "(Supplement)" what does this refer to? On that note: in the supplementary P1, L15, it reads that "a" is set to "2"? How do these two sections relate to each other? Is "a" estimated as described in eq. 2-3 or is it set to a constant value? Why would it be constant? I cannot find the motivation to set "a" to 2 in Goodman and Weare 2010.

Not in Goodman and Weare, but in Foreman-Mackey et al. This is changed in the supplement.

P7, L37: "$(IQR(R)/1.349)^2$": Please explain IQR (Inter-Quartile-Range?) and where the 1.349 is coming from.

Inter-Quartile Range. 1.349 is an adjustment factor to calculate sample standard deviation from the Inter-Quartile Range (Ghosh 2018, Silverman 1986).

P8, L4-6: See main comment 1. Yes, there can be more modes, but eventually there can only be as many change-points as allowed by the user (6+2). Please rephrase, and provide a short section (here or elsewhere in the manuscript) discussing differences arising from the choice of allowed change-points.

See the response above, to the longer comment. We discuss the difference arising from the choice of 7 or 8 change points at the ACR in the second paragraph of section 3.3, and provide fits with 5-9 points in the supplement. We also provide probability maxima and 65% / 95% confidence intervals for both 7 and 8 point fits in the supplementary spreadsheet.

P8, L8: "second derivative of the fits": I don't understand. The fits are straight lines, so the second derivative is always 0?

At the change points the first derivative is discontinuous and changes abruptly. We take into account the direction of this change. This is now worded "by the sign of the change in slope of the fits".

P8, L8-16: I do not understand what is done here. 1000 change points at once? Or 1000x1 random change-point? Or 1000 x (6+2) random change-points? How do the histograms reflect the approximate slope? Please clarify this section.

This section is no longer included, as we have removed the vertical probability threshold.

P9, Figure caption 3: Line 3, typo "Rrobability"; Line 5: "the sum" - linear? Quadrature?

Accepted. Changed to quadratic sum.

P9, L36: "one at the ACR onset": see main comment 4 – this is impossible to see.

Revised. The histograms in the figures now do not overlap with the time series.

P10, L44-45: see main comment 4 – impossible to see.

Revised. The histograms in the figures now do not overlap with the time series.

P10, L48-49: "roughly concurrent with the downward CO2 change point" replace with "concurrent with the second mode of the downward CO2 change point" Also, this statement is at odds with P12, L16, where you state, that you do not identify a CO2 change-point. Please check for consistency.

In the 7-point fit, there is only one mode of the CO2 change point.

P10, L1 (50?, line-numbering is off): "No corresponding change point is detected for CO2". This is briefly discussed in section 3.2 but maybe it is already here worthwhile mentioning that this change point is only present in East Antarctic temperature records?

We prefer to keep the analysis of the stack and individual records separate, to avoid confusion for the reader.

P10, L4: "The Holocene onset is well defined". I suppose the way the Holocene is defined it cannot be seen in Antarctic isotope records. Maybe replace with "The end of the deglacial warming is well-defined.."

Accepted "The end of the deglacial warming in Antarctica." This is replaced, in general, with the terminology "deglaciation end" or "T1 end".

P10, L10-13: See main comment 2.

Revised

P11, L24: See earlier – is Bintanja et al. 2013 the correct reference?

As above, we now fit individual d18O records, in accordance with Buizert et al. (2018). This does not significantly change the result.

P11, L30: "rather broad, non-significant". That is by design. See comment 1. Maybe change to: "rather broad and hence, non-significant."

The probability threshold no longer used; hence, we no longer assess significance.

P12, L41: "... with temperature change at WD appearing to slightly precede temperature in the East Antarctic records,... ". Omit the second use of "temperature" or change to "temperature change"

Revised (now d18O)

Figure 6: The PDFs in the top-left and bottom-right panels are the same plot. Please check/replace.

These are replaced with new PDFs.

Figure 6 and throughout this section: See main comment 3.

Revised

P13, L4-5: Mention again, that interestingly this is not the case for Dome Fuji?

Accepted. This is included in section 3.2.

P13, L12: Mention again that the 14k change-point is not present everywhere?

Accepted. Included in section 3.2.

P14, L15-16: "was most likely synchronous" change to: "occurred within xx years of the CO2 change"

Replaced with "we cannot calculate a clear lead of either ATS3 or CO2" due to the large uncertainty regarding this change.

P14, L16-17: "Further, we do not identify an analog in CO2 of the marked temperature decrease…". But figure 3 and 4 do show downward histograms there? As mentioned in main comment 1, I think this is related to how significance is defined. There seems to be a downward change-point that is just not very well constrained in time, and hence, yields a low and wide probability distribution. See also earlier comment – check for consistency with P10, L48-49.

This is an error, now reads "of the temperature stabilization"

P14, L37: Within error also the ACR onset "allows" for the CO2-ATS phasing to be reversed. And for both events, phasing is zero within error.

This is the case at the 95% level. In accordance with a comment from Reviewer 2, revised to "our results allow for the CO2-ATS3 phasing to be different during the two events, with the maximum probabilities reversed in directionality (i.e. with temperature leading at T1 and CO2 leading at the ACR end, though zero phasing is within 95% error)"

P14, L38: "But the phasings are opposite in direction and different in magnitude": This sentence is unclear. Do you mean that CO2 and CH4 change in opposite directions? Why is it relevant that the magnitude of CO2 and CH4 change differs, and how do you define the magnitude for 2 gases that have very different background concentrations?

Rephrased to: "Though CH4 appears to change alongside CO2 during both intervals, the phasings between CO2 and Temperature during the intervals are opposite in direction and different in slope."

P14, L42: "None of the five isotopic records show significant probability in this region" change to: "We do not detect a significant change-point for any of the isotope records during this period."

Accepted

Figure 7: Please also add a dashed vertical line to the oldest change-point/Mt. Takahe eruption that extends through all panels.

P15, L3: "only roughly consistent" Can you please be more precise?

We have replaced this with an assessment of each change point.

P15, L11, "ice-air shift" Please replace with "delta-age"

Accepted.

P16, L21. Also add, that the end of deglacial warming occurs later in DF?

Accepted

Reviewer 2

Review of Chowdhry Beeman et al. *The manuscript has had major revisions and is improved. However, more work is in my view still needed to justify some of the conclusions (see major points). I also have a rather long list of more technical points that need to be clarified or corrected.*

Major points

Regarding the phasing differences between temperature and CO2 at different Antarctic sites. The discussion of these results is very brief and the statement in the conclusions "we confirm that the deglacial temperature rise did not occur homogeneously across the Antarctic continent" is in my opinion not yet justified. It would help a great deal to include a table which shows the phasing results and uncertainties for the stack and for the individual cores for each change point. Then we could more easily see if the phasing differences are indeed significant and at what level.

Accepted. We have now included such a table (timings and phasings for each core) in the supplementary spreadsheet.

I am not completely convinced by the method to assess uncertainty in the phasing estimates. The additional comments in the supplement on significance testing largely repeat what is already in the main text. One way to test this and convince this reviewer and readers would be to trial the method on some artificial data with known change points and AR(1) noise.

This is now present in the supplementary materials.

In comparing the lag results with other studies the authors use qualitative language like 'nearly.. roughly consistent.. etc'. Please use more quantitative language. For example the phasing at T1 in Parrenin et al was -10± 160 years and here it is 449 ± 257 years. This needs some more explanation than 'only roughly consistent'. If these results are indeed to be a target for carbon cycle modeling, then we need to be confident that this number will not change again in several years, can we be? Please address this concern in the revised text.

The phasings will be addressed in terms of probability (now included in the abstract, section 3.3, Table 1, and the supplementary spreadsheet).

However, we must accept that the numbers and uncertainty ranges for phasings may indeed change in several years (and so should modelers of the carbon cycle). As the reviewers know very well, paleoclimatology is a dynamic field, and new CO2 measurement methods, used on high-resolution cores, better source corrections for temperature isotopes, the inclusion of more highly-resolved temperature records from new drilling sites, and last but certainly not least better methods for addresing phasing! could all change the lead-lag estimates. Our ranges of uncertainty are by design relatively large (we attempt to account for as many sources of uncertainty as possible, including AR1 noise that may obstruct the detection change points), so new estimates will very likely fall within our ranges. These rather large ranges can provide an appropriate target for carbon cycle modelers. But advances and improvements are at the core of scientific investigation. So, at least the first author of this paper profoundly disagrees, in principle, that the numbers regarding the phasing between CO2 and Antarctic temperature records should not change again. Indeed, they should be revised as new records are developed, although hopefully the confidence intervals should stay compatible.

Technical points

Abstract. List the lead/lag and uncertainties for the four coherent changes instead of using ambiguous terms like 'nearly' and 'most likely led'. The note in the supplement indicates that the lags are near Gaussian so I can't see why not to report as such. Or, if you have a strong rationale for avoiding quantitative descriptions then make that argument clearly in the text.

The probability ranges are asymmetric, as noted by the first reviewer. Inserted.

Some description, though, helps a probability distribution become understandable, so we don't want to categorically give up on describing the distributions quantitatively.

Line 9. For clarity drop "During the large, millenial-scale changes".

Accepted (in the abstract).

Line 11. Again, give the lead/lag and uncertainty.

Accepted (in the abstract).

Line 30. The ACR occurs midway (in time) through the deglaciation, not 'near the end'.

Accepted (in the introduction). Now reads "midway through".

P2 L35: missing citation.

Added Anklin et al., 1995.

P2 L38: Marcott 2014 does not present evidence of increased Southern Ocean upwelling during the deglaciation as far as I'm aware. Better would be Anderson et al., Science 2009 and Skinner et al., Science, 2010.

Accepted

P3L35-36: No. The study used Byrd and Siple CO2 data not Law Dome CO2 data.

Modified accordingly.

P3L39: "Roughly in phase.. etc'. No, instead list the lag and uncertainty for the intervals mentioned in this sentence.

Accepted, but we still think it is important to give the reader an idea of the phasing that is easy to retain in the introduction. So descriptions will be left in the text alongside the phasing.

P4L5: and others?

Latex compilation error, deleted.

P4L6: You mean during the satellite era?

Yes, the directly observed (not paleoclimate proxy) record. Accepted.

P4L24: "The standard deviation of the records at each timestep is assumed to be representative of the uncertainty concerning the conversion from isotopes to temperature,"... No I do not agree with this. Clarify or drop.

Deleted

P5L35: This sentence is unclear, please revise.

Changed to:
We identify likely change points using piecewise linear functions. Residuals are calculated between linear functions with a fixed number of stochastically proposed change points, which are free to explore the entire temporal range of the time series, and the raw data (similarly to Parrenin et al. (2013)). These residuals form a cost function, which allows us to perform a Bayesian analysis of the probable timing of change points.

P7L36: Python

Accepted

Fig 3 caption, L3: Probabilities.

Accepted

Fig 3: The dotted lines are a good addition. The caption should refer the reader to the relevant section of the text to understand where this threshold comes from.

The threshold is no longer used, in accordance with the second reviewer's new round of comments.

P8L18: The choice of the .0003 threshold over the..

The threshold is no longer used, in accordance with the second reviewer's new round of comments.

Fig 6. Caption: is the blue text including the result for the equivalent change point in Parrenin et al.,? Clarify in the caption.

Accepted, this is now moved to Table 1.

The result for deglacial onset appears substantially different to Parrenin et al. i.e. 10±160 yr CO2 lead (Parrenin) to 449±257 yr ATS2 lead (this work). Some specific comments on the main source of this timing difference are needed.

The following will be included:

The considerable difference at T1 between our result and that of Parrenin et al. (2013) is most likely due to the much higher resolution of the WAIS Divide CO2 time series. It is also possible, that the result of Parrenin et al. (2013) was limited to a local probability maximum of this change point in the CO2 series.

P14L37: 'Though the T1 onset and the ACR end are both thought to originate in AMOC reductions (Marcott et al., 2014), our results allow for the CO2 - ATS2 phasing to be reversed during the two events (i.e. with temperature leading at T1 and CO2 leading at the ACR end).'

Accepted. In accordance with a comment from reviewer 1 This is now "our results allow for the CO2-ATS3 phasing to be different during the two events, with the maximum probabilities reversed in directionality (i.e. with temperature leading at T1

and CO2 leading at the ACR end, though zero phasing is within 95% error)"

P14L37: "CH4 changes nearly synchronously with CO2 at both points, but the phasings are opposite in direction and different in magnitude." What is the basis for this statement? You did not assess CH4 phasing.

Rephrased to: "Though CH4 appears to change alongside CO2 during both intervals, the phasings between CO2 and Temperature during the intervals are opposite in direction and different in slope."

Pl5 L4:" Within the range of uncertainty, our lead-lag estimates are only roughly consistent with those of Pedro et al. (2012) and Parrenin et al. (2013)." They are either consistent or they are not - use precise language.

Worded as below.

"Within the range of uncertainty, the mean of our lead-lag estimates is consistent with the boundaries proposed by Pedro et al. (2012). Our results are consistent with those of Parrenin et al. (2013) for three out of the four change points addressed, but differ considerably at the T1 onset."

*P14L35... Add some words to clarify this result: "However, the cumulative probability of the ATS2 change point is much greater before 17.7 ka than after (*see Figure 7*); hence our results are do not support McConnell et al's proposed volcanic forcing of the temperature change.*

Accepted.

P14L47: suggest to cite here Buizert et al., Nature, 2018 (https://doi.org/10.1038/s41586-018-0727-5) which finds that EDML has a consistently different atmospheric response to AMOC perturbations than other Antarctic records. Being geographically closer to the Atlantic does not necessarily imply EDML should resolve Atlantic temperature anomalies with more fidelity than other cores, the reason is the ACC barrier, which anomalies must mix across to enter the polar ocean; this likely happens to a large extent down-stream of the Atlantic sector (see Pedro et al., 2018, https://doi.org/10.1016/j.quascirev.2018.05.005).

Accepted, we also now use the d18O stack from Buizert et al. (2018). This now reads "EDML indeed appears to record changes in AMOC differently than the other isotopic records (Landais et al., 2018; Buizert et al., 2018).

P16 L15: "This variability suggests complex mechanisms of coupling that can be modulated by external forcing". Expand on what you mean by this, why should the modulation be external and not internal? As it stands this statement is not justified and not convincing.

Reworded:

"This variability of phasings indicates that the mechanisms of coupling are complex. We propose three possibilities: I) the mechanisms by which CO2 and Antarctic Temperature were coupled were consistent throught the deglaciation, but can be modulated by external forcings or background conditions that impact heat transfer and oceanic circulation (and hence CO2 release); II) these mechanisms can be modulated by internal feedbacks that change the response timings of the two series; and/or III) multiple, distinct mechanisms might have provoked similar responses in both series, but with accordingly different lags."

Figure 5: This was a very good addition, but plotting time series around the map, makes the panels much too small. I suggest a standard layout with the map above or below.

This figure is revised.

P16 L17: .. between West and East Antarctica. . .

Can the comment be clarified?

P16 L18: what is meant by 'regional external influences'? Influences other than regional temperature?

"is complicated by influences other than regional temperature, including source temperature and ice sheet elevation change"

P16 L20: be more precise about what these differences are and why you think they are significant and at what level (a Table comparing the results for all sites would help).

Accepted, a spreadsheet is now included in the supplement.

P16 L24: drop 'as is the investigation of the role CO2 in global temperature change.' It is repeated further down.

Accepted

Supplement: The note on Gaussian uncertainties should be moved to the main text. The note on assessing significance is central to the results and should also be integrated into the main text (and see major comments above).

These points have now been changed, in accordance with reviewer one's comments.

Antarctic temperature and CO_2: near-synchrony yet variable phasing during the last deglaciation

Jai Chowdhry Beeman[a,1], Léa Gest[a,1], Frédéric Parrenin[a], Dominique Raynaud[a], Tyler J. Fudge[b], Christo Buizert[c], and Edward J. Brook[c]

[a]Univ. Grenoble Alpes, CNRS, IRD, IGE, F-38000 Grenoble, France
[b]Department of Earth and Space Sciences, University of Washington, Seattle, WA 98195, USA
[c]College of Earth, Ocean, and Atmospheric Sciences, Oregon State University, Corvallis, OR 97331, USA
[1]Jai Chowdhry Beeman and Léa Gest contributed equally to this work.

Correspondence to: Frédéric Parrenin frederic.parrenin@univ-grenoble-alpes.fr

Abstract. The last deglaciation, which occurred from 18,000 to 11,000 years ago, is the most recent large natural climatic variation of global extent. With accurately dated paleoclimate records, we can investigate the timings of related variables in the climate system during this major transition. Here, we use an accurate relative chronology to compare temperature proxy data and global atmospheric CO_2 as recorded in Antarctic ice cores. In addition to five regional records, we compare a $\delta^{18}O$ stack, representing Antarctic climate variations, with the high-resolution, robustly dated WAIS Divide CO_2 record. We assess the CO_2 / Antarctic temperature phase relationship using a stochastic method to accurately identify the probable timings of ~~abrupt~~changes in their trends. Four coherent changes are identified for the two series, and synchrony between CO_2 and temperature is within the 95% uncertainty range for all of the changes except the end of Termination 1. During the ~~large, millenial-scale changes at the~~ onset of the last deglaciation at 18 ka and the deglaciation end at 11.5 ka, Antarctic temperature

most likely led CO_2 by several centuries (by 570 years, within a range of 127 to 751 years, 68% probability, at the T1 onset; and by 532 years, within a range of 337 to 629 years, 68% probability, at the deglaciation end). At 14.4 ka, the onset of the Antarctic Cold Reversal (ACR) period, our results do not show a clear lead or lag (Antarctic temperatre leads by 50 years, within a range of -137 to 376 years, 68% probability). The same is true (CO_2 leads by 65 years, within a range of 211 to 117 years, 68% probability) at the end of the ACR. However, the timings of changes in trends for the individual proxy records show variations from the stack, indicating regional differences in the pattern of temperature change, particularly in the WAIS Divide record at the onset of the deglaciation; the Dome Fuji record at the deglaciation end; and the EDML record after 16 ka. In addition, two significant changes, one at 16 ka in the CO_2 record and one after the ACR onset in three of the isotopic temperature records, do not have significant counterparts in the other record. The likely-variable phasings we identify testify to the complex nature of the mechanisms driving the carbon cycle and Antarctic temperature during the deglaciation.

1 Introduction

Glacial-interglacial transitions, or deglaciations, mark the paleorecord approximately every 100,000 years over the past million years or so (Jouzel et al., 2007; Lisiecki and Raymo, 2005; Williams et al., 1997). The last deglaciation, often referred to as glacial termination 1 (T1), offers a case study for a large global climatic change, very likely in the 3 - 8°C range on the regional~~global~~ scale (Masson-Delmotte et al., 2013), and thought to be initiated by an orbitally driven insolation forcing (Berger, 1978; Hays et al., 1976; Kawamura et al., 2007). The canonical interpretation of this apparent puzzle is that insolation acts as a pacemaker of climatic cycles and the amplitude of glacial - interglacial transitions is mainly driven by two strong climatic feedbacks: atmospheric CO_2 and continental ice surface - albedo changes. However, the mechanisms that control the CO_2 rise are still a matter of debate. Accordingly, reconstructing the phase relationship (leads and lags) between climate variables and CO_2 during the last termination has become of importance, and has a substantial history in ice core research (Barnola et al., 1991; Caillon et al., 2003; Parrenin et al., 2013; Pedro et al., 2012; Raynaud and Siegenthaler, 1993).

Global temperature has been shown to lag CO_2 on average during T1 (Shakun et al., 2012), supporting the importance of CO_2 as an amplifier of orbitally-driven global-scale warming. But Antarctic temperature and CO_2 concentrations changed much more coherently as T1 progressed. Indeed, midway through the glacial-interglacial transition, Antarctic warming and CO_2 increase slowed and even reversed during a period of about 2000 years, coinciding with a warm period in the North called the Bølling–Allerød (B/A). ~~this~~The respective period of cooling in Antarctica is called the Antarctic Cold Reversal (ACR). A period of cooling in the Northern Hemisphere known as the Younger Dryas (YD), followed the B/A, coinciding with a period of warming in the SH.

High-latitude Southern Hemisphere paleotemperature series–including Southern Ocean temperature–varied similarly to Antarctic temperature during T1 (Shakun et al., 2012; Pedro et al., 2016). Upwelling from the Southern Ocean is thought to have played an important role in the deglacial CO_2 increases (Anderson et al., 2009; Burke and Robinson, 2012; Rae et al., 2018; Schmitt et al., 2012). The Atlantic Meridional Overturning ~~Current,~~ or AMOC, a major conduit of heat between the Northern and Southern Hemispheres and component of the bipolar seesaw, the umbrella term encompassing the mecha-

nisms thought to control the seemingly alternating variations of Northern and Southern Hemisphere temperature (Stocker and Johnsen, 2003; Pedro et al., 2018), is thought to have influenced Southern Ocean upwelling during the deglaciation (Anderson et al., 2009; Skinner et al., 2010). A weakening of the oceanic biological carbon pump appears to have dominated the deglacial CO_2 increase until 15.5 ka, when rising ocean temperature likely began to play a role as well (Bauska et al., 2016).

Ice sheets are exceptional archives of past climates and atmospheric composition. Local temperature is recorded in the isotopic composition of snow/ice (Jouzel et al., 2007; NorthGRIP Project Members, 2004) due to the temperature dependent fractionation of water isotopes (Lorius and Merlivat, 1975; Johnsen et al., 1989). ~~The concentration of continental dust in ice sheets is a proxy of continental aridity, atmospheric transport intensity and precipitation. Finally,~~ Air bubbles enclosed in ice sheets are near-direct samples of the past atmosphere. However, the age of the air bubbles is younger than the age of the surrounding ice, since air is locked in at the base of the firn (on the order of 70 m below the surface on the West Antarctic Ice Sheet (WAIS) Divide) at the Lock-In Depth (LID) (Buizert and Severinghaus, 2016). The firn, from top to bottom, is composed of a convective zone (CZ) where the air is mixed vigorously, and a diffusive zone (DZ) where molecular diffusion dominates transport. Firn densification models can be used to estimate the LID and the corresponding age difference (Sowers et al., 1992).

Atmospheric CO_2 concentrations, recorded in the air bubbles enclosed in ice sheets, are better preserved in Antarctic ice than in Greenland ice, because the latter has much higher concentrations of organic material and carbonate dust (Raynaud et al., 1993; Anklin et al., 1995). Measured on the Vostok and EPICA Dome C ice cores, the long-term history ~~ice core record~~ of CO_2 (Lüthi et al., 2008) covers the last 800 ka.

Early studies suggested that at the initiation of the termination around 18 ka B1950 (kiloyears before 1950 A.D.), just after the Last Glacial Maximum (LGM), Antarctic temperature started to warm 800 ± 600 yr before CO_2 began to increase (Monnin et al., 2001), a result that was sometimes misinterpreted to mean that CO_2 was not an important amplification factor of the deglacial temperature increase. This study used measurements from the EPICA Dome C (EDC) ice core (Jouzel et al., 2007) and a firn densification model to determine the air chronology. However, this firn densification model was later shown to be in error by several centuries for low accumulation sites such as EDC during glacial periods (Loulergue et al., 2007; Parrenin et al., 2012).

Two more recent works (Pedro et al., 2012; Parrenin et al., 2013), used stacked temperature records and improved estimates of the age difference between ice and air records to more accurately estimate the relative timing of changes in Antarctic temperature and atmospheric CO_2 concentration. In the first of these studies, measurements from the higher accumulation ice cores at Siple Dome and Byrd Station~~Law Dome~~ were used to decrease the uncertainty in the ice-air age shift, and indicated that CO_2 lagged Antarctic temperature by 0-400 yr on average during the last deglaciation (Pedro et al., 2012). The second study (Parrenin et al., 2013) used measurements from the low accumulation EDC ice core but circumvented the use of firn densification models by using the nitrogen isotope ratio $\delta^{15}N$ of N_2 as a proxy of the DZ height, assuming~~hypothesizing~~ that the height of the CZ was negligible during the study period. CO_2 and Antarctic temperature were found to be in phase at the beginning of TI (-10 ± 160 years) and at the end of the ACR period (-60 ± 120 years), but CO_2 was found to lag Antarctic temperature by several centuries at the beginning of the Antarctic Cold Reversal (260 ± 130 years) and at the end of the deglacial warming in Antarctica (500 ± 90 years). The end of the deglacial warming in Antarctica occured roughly two

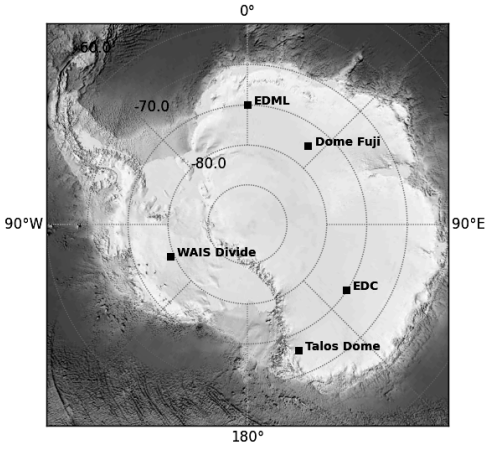

Figure 1. Drilling locations of the ice cores from which the CO_2 and isotopic paleotemperature records included in this study were measured.

centuries after the onset of the Holocene period, dated at 11.7 ka according to the International Commission on Stratigraphy. However, the assumption that $\delta^{15}N$ reflects DZ height is imperfect, as it may underestimate the DZ height for sites with strong barometric pumping and layering (Buizert and Severinghaus, 2016).

A new CO_2 record of unprecedented high resolution (Marcott et al., 2014) from the WAIS Divide (WD) ice core merits the reopening of this investigation. The air chronology of WAIS Divide is well constrained thanks to a relatively high accumulation rate and to accurate nitrogen-15 measurements (Buizert et al., 2015). The WAIS record evidences centennial-scale changes in the global carbon cycle during the last deglaciation superimposed on more gradual, millenial-scale trends that bear resemblance to Antarctic temperature (Marcott et al., 2014).

The deglacial temperature rise seen at WD is structurally similar to that at other Antarctic sites. However, West Antarctic warming may have been greater in magnitude than East Antarctic warming by up to 3 degrees, and the rise in West Antarctic temperature shows an early warming starting around 21 ka B1950, following local insolation (Cuffey et al., 2016). This early warming trend is much more gradual in records from East Antarctic ice cores. The difference between the two records may be ~~related with~~related to sea ice conditions around East and West Antarctica, and perhaps to elevation changes (Cuffey et al., 2016; WAIS Divide Project Members, 2013). ~~However,~~ The temperature record at WAIS Divide shows an acceleration in warming around 18 ka B1950 which is also present in East Antarctic records (WAIS Divide Project Members, 2013).

On the much shorter timescales of the satellite era, Jones et al. (2016) note differing temperature trends at the drilling sites of the five cores used in this study. On the other hand, the interpretation of individual isotopic records can prove complicated, as local effects, including those of ice sheet elevation change and sea ice extent, are difficult to correct.

In the present work we refine our knowledge of leads and lags between Antarctic temperature and CO_2. We use a stack of accurately synchronized Antarctic temperature records (Buizert et al., 2018) to reduce local signals, placed using volcanic

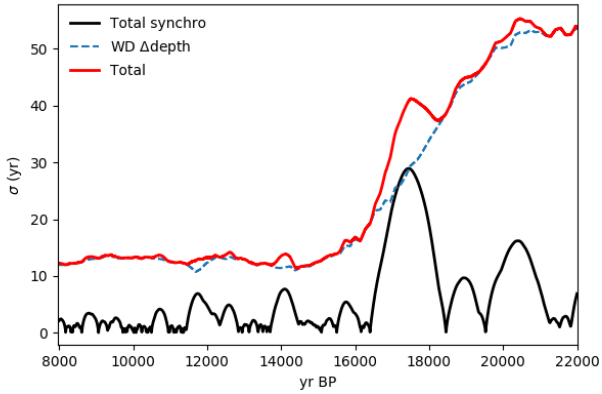

Figure 2. Relative chronological uncertainty between ATS3 and the WD CO_2 record (red line), calculated as the quadratic sum of the synchronization error from Buizert et al. (2018) (black line) and the Δ age uncertainty from WD2014 (blue dashed line).

.

matching on the WAIS Divide chronology (WD2014). We then compare the temperature stack to the high resolution WAIS Divide CO_2 record by determining the probable timings of changes in trend, and calculate probable change point timings for the five individual isotope-derived records used in the stack as well.

2 Methods and data

2.1 Temperature stack and ice chronology

We use the $\delta^{18}O$ stack developed by Buizert et al. (2018) (referred to hereafter as Antarctic Temperature Stack 3, or ATS3) to represent Antarctic Temperature. The use of the stack allows us to remove local influences and noise in the individual records to the greatest extent possible. The stack contains five records: EDC, Dome Fuji (DF), Talos Dome (TALDICE), EPICA Dronning Maud Land (EDML) and WAIS Divide (WD). Volcanic ties between WD and EDC, WD and TD, and WD and EDML are developed in Buizert et al. (2018); previously published volcanic ties were used between EDC and DF (Fujita et al., 2015), placing all of the records on the WD2014 chronology (Buizert et al., 2015). Notably, the Vostok record, included in the stack used by Parrenin et al. (2013) is excluded from the Buizert et al. (2018) stack: it contains additional chronological uncertainty as it is derived using records from two drilling sites. We take the quadratic sum of the synchronization error from Buizert et al. (2018) and the Δ age uncertainty from WD2014 to calculate the relative chronological error between ATS3 and the WD CO_2 record.

2.2 CO_2 and air chronology

We use atmospheric CO_2 data from the WD ice core (Marcott et al., 2014) which consist of 1,030 measurements at 320 depths that correspond to ages between 23,000 and 9,000 years B1950 with a median resolution of 25 years. At WD, the age offset between the ice and air ~~(trapped much later)~~ at a given depth, Δage, is calculated using a firn densification model, which is constrained using nitrogen-15 data, a proxy for firn column thickness (Buizert et al., 2015). Δage ranges from 500 ± 100 yr at the last glacial maximum, to 200 ± 30 yr during the Holocene. Δage uncertainty is added to cumulative layer counting uncertainty to determine the total uncertainty of the air chronology.

2.3 Identifying changes in trend

We identify likely change points using piecewise linear functions. Residuals are calculated between linear functions with a fixed number of stochastically proposed change points, which are free to explore the entire temporal range of the time series, and the raw data (similarly to Parrenin et al. (2013)). These residuals are summed to form a cost function, which allows us to perform a Bayesian analysis of the probable timing of change points. At the base of our method is a parallelized Metropolis-Hastings (MH) procedure (Goodman and Weare, 2010; Foreman-Mackey et al., 2013). Therefore, we do not present a single "best fit" but rather analyze the ensemble of fits accepted by the routine. We plot two histograms: an upward-oriented histogram for concave-up change points, and a downward-oriented histogram for concave-down change points. We use these histograms as probabilistic locators of changes in slope (Figure 3).

The change point representations of the ATS3 and CO_2 time series are composed of a set of n specified change points $\{\boldsymbol{X}_i = (x_i, y_i) |\ i = 1, \ldots, n\}$. We denote the vector of m time series observations o at time t $\{\boldsymbol{O}_l = (t_l, o_l) |\ l = 1, \ldots, m\}$, and the scalar residual term J between observations and the linear interpolation between change points f_y:

$$J(\boldsymbol{X}_i) = \boldsymbol{R}^T \mathbf{C}^{-1} \boldsymbol{R};\ \boldsymbol{r}_l = \left(f_y(t_l) - o_l\right)_l \tag{1}$$

where $\boldsymbol{R}$ is the vector of residuals at each data point with components $\boldsymbol{r}_l$ and $\mathbf{C}$ is the covariance matrix of the residuals. The ATS3 series contains 700 data points, and the WD CO_2 series contains 320, each of which is considered in the residuals.

We fix $x_0 = t_0$ and $x_n = t_l$; i.e. the x-values of the first and last change points are fixed to the first and last x-values of the observation vector, with the y-values allowed to vary. The remaining points are allowed to vary freely in both dimensions.

2.3.1 Estimating the covariance matrix C: treating uncertainty and noise

Our method fits time series with piecewise linear functions, and the residual vector thus accounts for any variability that cannot be represented by these fits. Paleoclimate time series, like the CO_2 and ATS3 series used here, typically contain autocorrelated noise (see Mudelsee (2002), for example) which cannot be accurately represented by a piecewise linear function. Weighting the residuals of a cost-function based formulation by a properly estimated inverse covariance matrix ensures that this autocorrelated noise is not overfitted, and can improve the balance of precision and accuracy of the fits.

Our time series contain two potential sources of uncertainty: measurement or observational uncertainty, related with the creation of the data series, and modeling uncertainty, related to the formulation of the fitting function. We formulate a separate covariance matrix to account for each source of uncertainty. These matrices are then summed to form $\mathbf{C}$. We assume ~~the first sourcethe~~ measurement uncertainty to be uncorrelated in time (i.e. a white noise process). Thus, the associated covariance matrix $\mathbf{C}_{meas}$ is diagonal, and the diagonal elements $\mathbf{C}_{jj}$ are each equal to the variance of observation o_j, σ_j^2, as estimated during the measurement process.

The covariance matrix of the modeling uncertainty, which we denote $\mathbf{C}_{mod}$, is more complicated, since the residual vector contains any autocorrelated noise in the time series that is not accounted for by the piecewise linear fits. Additionally, the time series contain outliers with respect to these linear fits, and these can impact any non-robust estimate of covariance. Finally, an initial idea of the model must be used to calculate residuals, and thus estimate their covariance. These challenges can be circumvented when data resolution is low enough to assume that residuals are uncorrelated, as in Parrenin et al. (2013), however, including the covariance matrix allows us to make use of noisy, high-resolution data.

We arrive at an initial model by running a MH simulation in which $\mathbf{C}$ is assumed equal to the identity matrix, and select the best fit of this run. Note that $\mathbf{C}_{meas}$ is not taken into account at this point, since we require an independent estimate of $\mathbf{C}_{mod}$. At this point, covariance could be estimated directly, but tests indicated that this method was not robust, making the covariance matrix estimate sensitive to outliers and to the initial model fit. Our CO_2 data are unevenly spaced in time, and developing a covariance matrix using the traditional covariance estimator would require some form of interpolation, which can introduce substantial error.

The residuals with respect to the initial model are instead used to fit an AR(1) model (Robinson, 1977; Mudelsee, 2002) which treats the autocorrelation between a pair of residuals r_i and r_{i-1} as a function of the separation between the two data points in time $t_i - t_{i-1}$. The Robinson (1977) / Mudelsee (2002) model is expressed as follows:

$$r_i = r_{i-1} \cdot a^{t_i - t_{i-1}} \tag{2}$$

where the constant a determines the correlation between two residuals separated by $t_i - t_{i-1}$ units of time, and minimizing the loss function:

$$S(a) = \sum_{i=1}^{n} \left\{ r_i - r_{i-1} \cdot a^{t_i - t_{i-1}} \right\} \tag{3}$$

allows us to estimate a. We do so using a nonlinear least-squares estimate with L1-norm regularization to provide a robust estimate (Chang and Politis, 2016). We ~~confirm~~test the validity of the AR(1) hypothesis by comparing r_i with $r_{i-1} \cdot a^{t_i - t_{i-1}}$ (Supplement). Given that the AR(1) hypothesis ~~is accurate~~cannot be rejected, we can use a to calculate the theoretical correlation between two residuals, and construct a correlation matrix $\mathbf{K}$ and the model covariance matrix $\mathbf{C}_{mod}$ as follows:

$$\mathbf{C}_{mod} = \sigma_{mod}^2 \, \mathbf{K} \; ; \; \mathbf{K}_{ij} = a^{t_j - t_i} \tag{4}$$

where σ^2_{mod} is the variance of the modeling error, assumed constant and estimated using a robust estimator based on the Interquartile Range (IQR), calculated as $(IQR(\mathbf{R})/1.349)^2$ (Ghosh, 2018; Silverman, 1986). Finally, the covariance matrix of the residuals C is calculated as:

$$\mathbf{C} = \mathbf{C}_{mod} + \mathbf{C}_{meas}. \quad (5)$$

Rather than inverting the covariance matrix, we use Cholesky and LU decompositions to solve for the cost function value J, as in Parrenin et al. (2015).

2.4 Estimating the posterior probability density

In general, the probability density of the change points cannot be assumed to follow any particular distribution, as short-timescale variations of the time series may lead to multiple modes or heavy tails, for example. Thus, stochastic methods, which are best adapted to exploring general probability distributions (for example, Tarantola (2005)), are suited to our problem.

To tackle the large computation time required for traditional MH sampling, we apply the ensemble sampler developed by Goodman and Weare (2010) (GW) as implemented in the Python emcee library (Foreman-Mackey et al., 2013). This sampler adapts the MH algorithm so that multiple model walkers can explore the probability distribution at once, making the algorithm parallelizable. It has the advantage of being affine invariant: that is, steps are adapted to the scale of the posterior distribution in a given direction.

The final task in our piecewise linear analysis is to identify the number of change points to best represent the two series we wish to analyze. The choice should reflect our goal of accurately investigating millenial-scale variability. Further, we aim for parsimony in the representation. To best balance these two goals, we apply the Bayesian Information Criterion (BIC, Schwarz et al. (1978)) to the number of points we allow to fit the two series.

We apply a joint BIC–normalizing the cost function for each series by its lowest value–and arrive at the conclusion that the two series are best compared by fitting 8 points. The histograms created for fits of 7, 8 and 9 points of the two series are remarkably similar, and we assess that our choice of 8 points does not add significant uncertainty to the timing of change points, with the exception of the change point at ACR onset. We include histograms of fits between 5 and 9 points in the supplementary materials. We also include change point timings and lead-lag estimates calculated using 7-point fits in the supplement.

The most probable timings are identified by probability peaks, or modes–for a fit of n points, we analyze the n time periods with greatest contiguous cumulative probability. Thus, we analyze a coherent number of change points, and avoid setting artificial probability thresholds. We avoid comparing incoherent modes by separating changes by the sign of the change in slope of the fits–that is, we compare concave-up changes with concave-up changes, and concave-down changes with concave-down changes. Further details of the simulations are given in the supplement.

2.5 Phasing

We estimate ρ_{lead}^{ATS3}, the probability that ATS3 leads CO_2 over a given interval, as

$$\rho_{lead}^{ATS3} = (\rho_x^{ATS3} \circ \rho_x^{CO_2}) \star \rho^{chron}, \tag{6}$$

where ρ_x^{ATS3} is the probability of a change point at time x for ATS3, $\rho_x^{CO_2}$ is the probability of a change point at time x for CO_2, $\circ$ is the cross-correlation operator, which is used to calculate the probability of the difference between two variables, and $\star$ is the convolution operator, which is used to calculate the probability of the sum of two variables. ρ^{chron} is the probability distribution of the chronological uncertainty between the two records, which we take to be Gaussian centered ~~on~~ 0, with standard deviation $\sigma = \sigma_{chron}$ (shown in Figure 3). The intervals associated with each change point are given in Figure 6.

3 Results and discussion

3.1 Change point timings

The change point histograms for the ATS3 and CO_2 time series in Figure 3 confirm that the millenial-scale changes in the two series were largely coherent. We focus on four major changes in trend which are common to both series: the onset of the deglaciation from 18.2 to 17.2 ka B1950; the onset of the Antarctic Cold Reversal (ACR) at around 14.5 ka, the ACR end beween 12.9 and 12.65, and the end of the deglaciation, at approximately 11.5 ka. For each of these four changes, we calculate the probability of a lead or lag over the time interval that encompasses the continuous peaks in the two histograms. Two CO_2 change points, one centered at approximately 16 ka, and one just before the ACR onset at 14.4 ka, do not have high-probability counterparts in the ATS3 series. A low-probability change point for the temperature series after the ACR onset, centered at 14 ka, does not have a counterpart in the CO_2 series.

The deglaciation onset begins with a large, postive change point mode for Antarctic temperature, centered around 18.1 ka. The corresponding change point for the CO_2 series is centered around 17.6 ka.

The CO_2 rise peaks at around 16 ka, identified by a downward-oriented probability peak, which has no significant counterpart in the temperature series. This peak is followed by a brief plateau in CO_2 concentrations, before a gradual, accelerating resumption of the increase.

At the onset of the Antarctic Cold Reversal, an upward-facing CO_2 change point at 14.4 ka is followed by a broad, downward-facing CO_2 change point which peaks at around 14.25 ka. The first peak appears to reflect a centennial-scale change (identified by Marcott et al. (2014)), and the broadness of the second peak reflects further methodological uncertainty with respect to the timing of the millenial-scale change in CO_2. An unambiguous negative temperature change also occurs at around 14.3 ka, roughly concurrent with the downward CO_2 change point. Antarctic temperature began to descend after the ACR onset, and it is worth mentioning the low-probability, concave-up change point mode centered on 13.9 ka, particularly because this point is much more probable for some of the individual isotopic record. No corresponding change point is detected for CO_2.

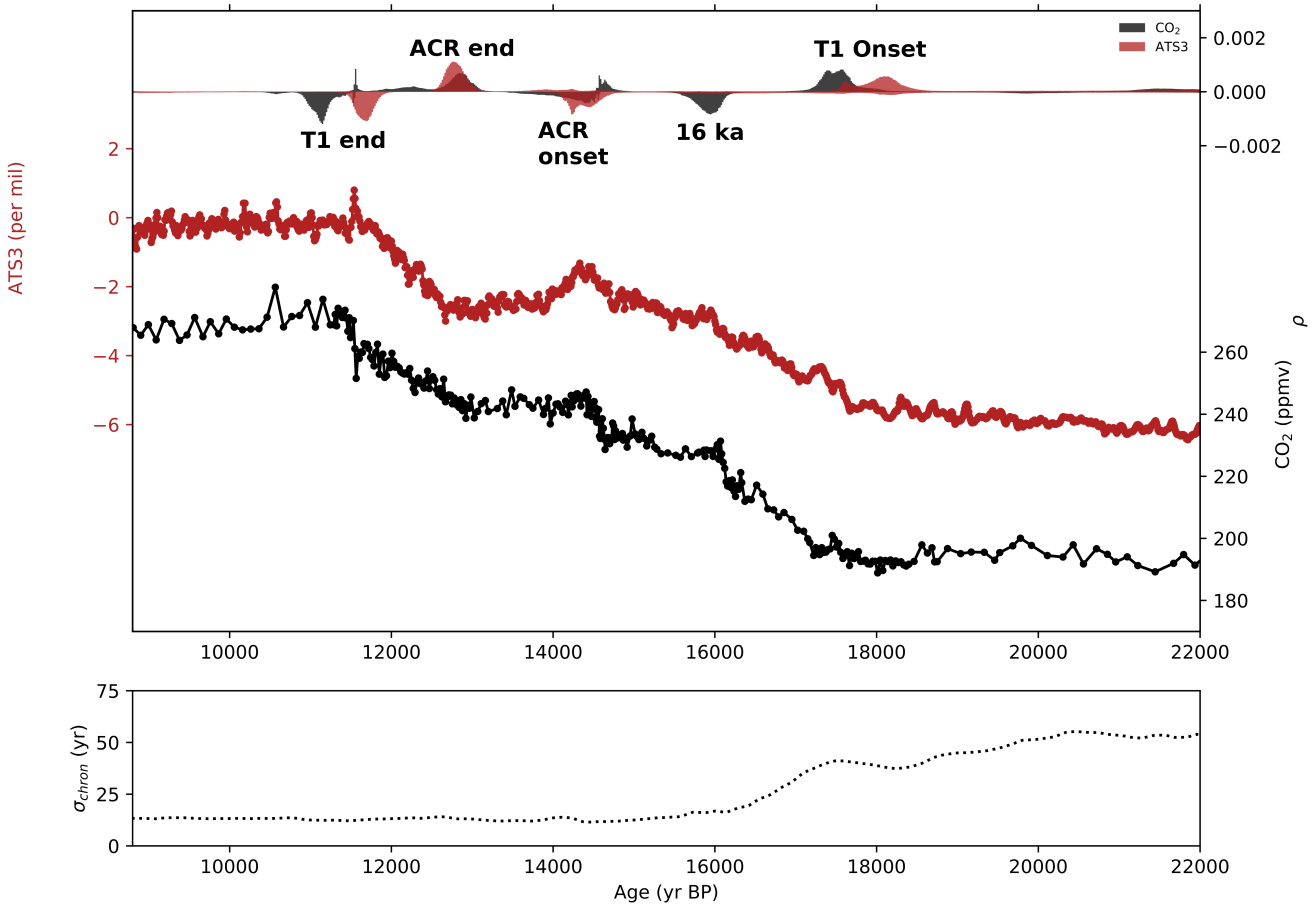

Figure 3. Upper panel: Atmospheric CO_2 (black) and ATS3 (red) placed on a common time scale, with the normalized histograms of probable change points (8 point simulations, allowed to fit 6 points and two endpoints per series). Histograms are plotted downward-oriented when the rate of change decreases and upward-oriented when it increases (same colors, y-axis not shown). Probabilities are normalized so that the integrated probability for a given histogram sums to 1, and range from 0 (center) to 0.004 (top/bottom). In four distinct time intervals, both series show concurrent probable change points. Lower panel: Chronological uncertainty, taken as the sum of the Δage uncertainties and the uncertainty estimate for our volcanic synchronization.

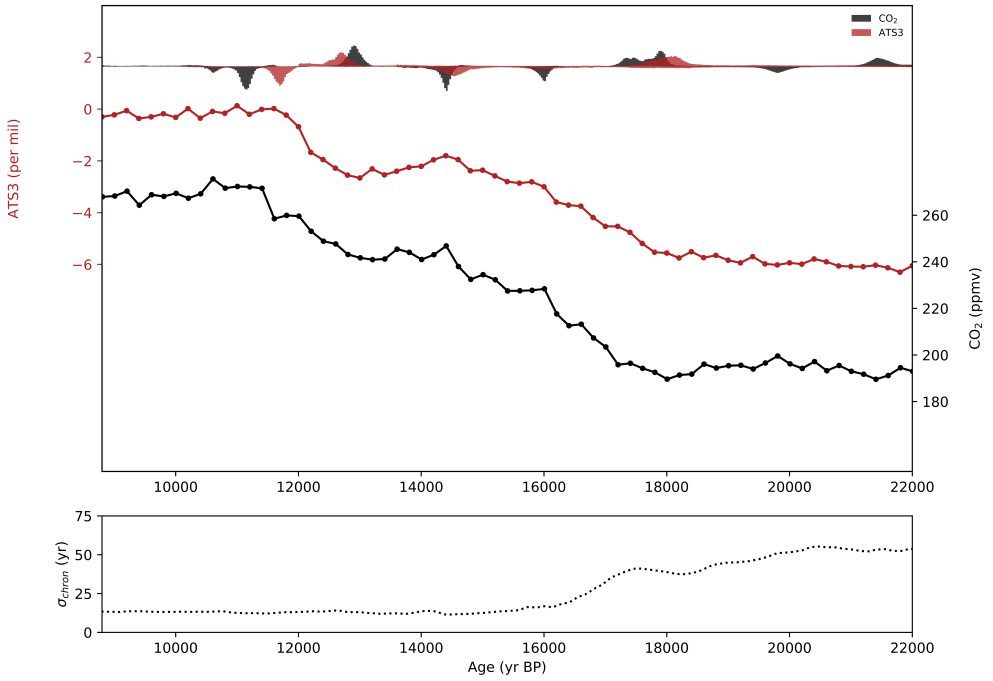

Figure 4. Upper panel: Savitsky-Golay filtered atmospheric CO_2 (black) and ATS3 (red) placed on a common time scale, with the normalized histograms of probable change points (8 point simulations, allowed to fit 6 points per series). Histograms are plotted downward-oriented when the rate of change decreases and upward-oriented when it increases (same colors, y-axis not shown, probabilities range from 0 (center) to 0.0024 (top/bottom)). Lower panel: Chronological uncertainty, taken as the sum of the Δage uncertainties and the uncertainty estimate for our volcanic synchronization.

The ACR termination is represented by significant modes in both series. An increase in CO_2 began at the peak occuring around 12.85 ka, while the ATS3 increase is centered at 12.78 ka, approximately, reaching its maximum around 12.7 ka.

The end of the deglacial warming in Antarctica is well-defined in the ATS3 series, with a large mode reaching its maximum at 11.7 ka. The corresponding CO_2 mode reaches its maximum at around 11.15 ka.

As a second test of the timings of millenial-scale events, we use our method to fit filtered versions of the ATS3 and WAIS Divide CO_2 data. A Savitsky-Golay filter, designed to have an approximate cutoff periodicity of 500 years, is applied to the two records. Fitting change points to these two series allows us to verify that our leads and lags are not overly influenced by sub-millenial scale noise in the original records.

Figure 4 shows the Savitsky-Golay filtered CO_2 and ATS3 time series, and the corresponding change point histograms. The four major changes identified in both series, at the T1 onset, the ACR onset, the ACR end, and T1 end, are similar in shape and center to the fits of the raw data. However, there are two notable differences between the two fits. First, the histograms are smoother and have broader peaks. This is not surprising, given that the Savitsky-Golay filters are designed to remove

all variability with periodicities less than 500 years, whereas the covariance matrix applied to the fits of the raw data only treats an approximation of AR(1) correlated noise. Second, the pre-ACR change in CO_2 is removed from the filtered series, which is again reasonable as it appears to mark a centennial-scale event. Savitsky-Golay filtering has its own drawbacks–data reinterpolation is required, for example, and propagating measurement uncertainty becomes difficult. However, the similarity of the two results supports our fits of the raw data.

3.2 Change point timings for individual temperature records

Fits of each of the regional $\delta^{18}O$ records are shown in figure 5. These fits should still be interpreted cautiously, as additional information included in the isotopic records here assumed to represent temperature–the signal of ice sheet elevation change, for example–are not corrected for. The comparison of these fits provides an initial, exploratory picture of potential regional differences in climate change during the last termination.

Of the four changes identified as coherent between the temperature stack and CO_2, those at the deglaciation onset, the ACR end, and the T1 end are expressed as significant probability peaks in all five records. Some ambiguity appears to exist about the timing of the ACR onset in the EDML record. It is expressed by a rather broad, non-significant probability mode extending between 16ka and 14ka, though a significant spike at 14ka marks the downturn seen in the other records. The ACR onset is significant and well-defined in all of the five other records. Three of the records–TD, EDC and WD–show a marked stabilization in temperature after the ACR onset, near 13.8 ka, which appears as a region of much lower probability in the ATS3 stack.

The WAIS Divide record is, notably, the only isotopic record in the stack from the West Antarctic ice sheet. We could thus reasonably expect it to show considerably different trends from the other records. Indeed, ~~a~~ changes in the WD temperature record occur at 22 ka and 20 ka. This earlier change in the isotopic record was identified and confirmed to indeed be a temperature signal by Cuffey et al. (2016) using a borehole temperature record, though their study places the change at 21 ka. We confirm that the onset of the deglacial temperature rise in West Antarctica likely began as much as 4 ka before the onset of temperature rise in East Antarctica. Interestingly, the WD record also shows a temperature change point around 17.8 ka, expressed slightly later than in the other records and more synchronous with CO_2. This apparent acceleration of the temperature rise is followed by a significant downward-facing change point not seen in any of the other records. A difference appears to exist in timing at the T1 end as well, with temperature change at WD appearing to precede the East Antarctic records, and the DF temperature change, centered at 11.2 ka, occuring more synchronously with CO_2.

3.3 Leads and lags

The probability densities of leads and lags at the coherent change points between ATS3 and CO_2 are shown in Figure 6. We ~~then~~ report the central 68% and 95% probability intervals for each histogram, thus avoiding any misinterpretation resulting from Gaussian approximation (mean and standard deviation). These values are grouped in Table 1.

ATS3 led CO_2 by 570 years, (within a 68% interval of 128 to 751 years) at the T1 onset. Given the large range of uncertainty, though, we cannot exclude the possibility of synchrony at the 95% level, which, interestingly, appears to be the case for the Dome Fuji record. At the ACR onset, we are not able to identify a clear lead or lag. At this point, phasing is sensitive to the

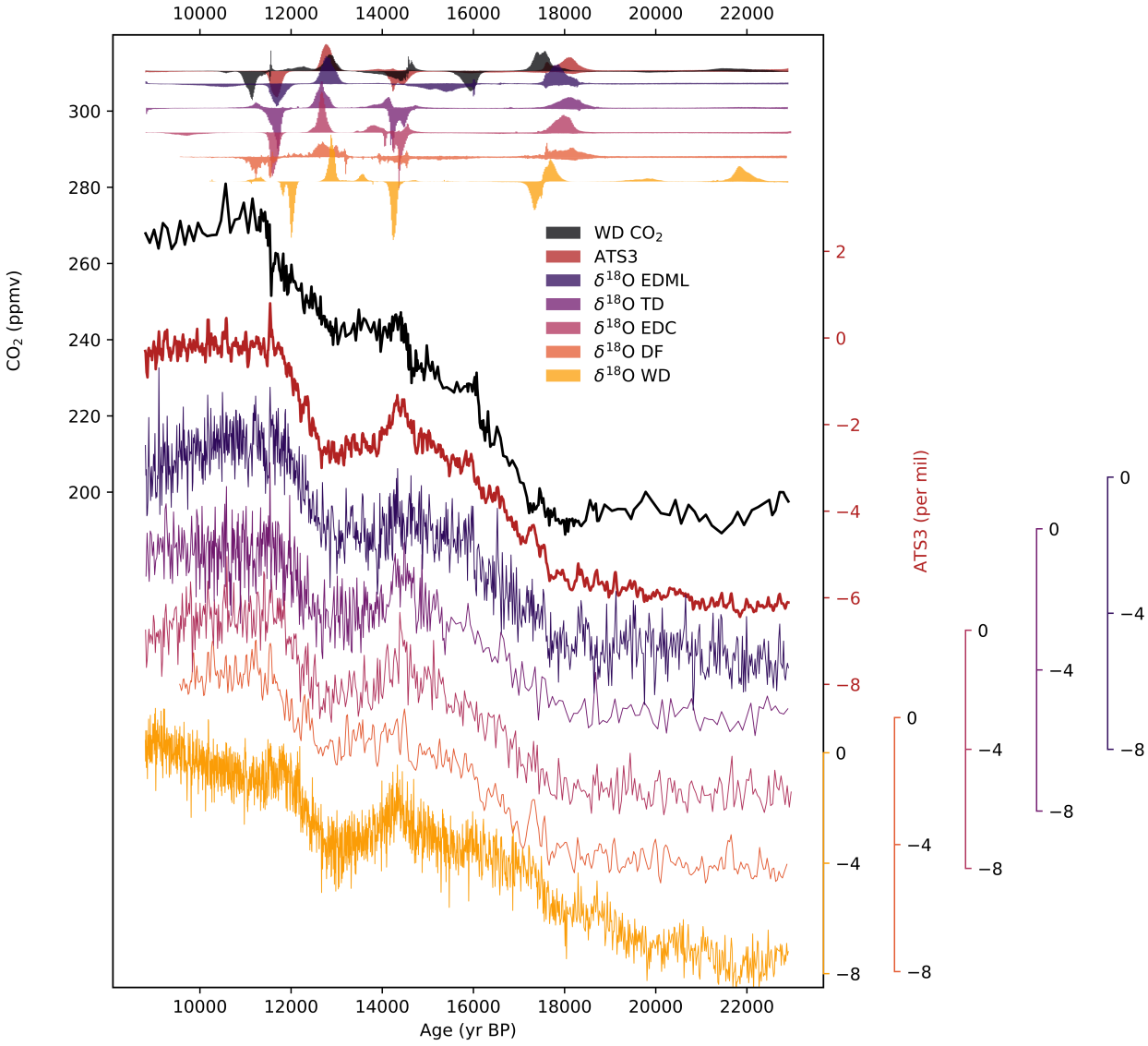

Figure 5. Atmospheric CO_2 (black) and individual $\delta^{18}O$ records placed on a common time scale, with the normalized histograms of probable change points (8 points) for each ice core used in the ATS3 stack; the locations of the drill sites are shown in ~~the top right corner.~~ Details of the histogram plots are as in Figure 3. Maximum probability estimates and 68/95% probability intervals for timings of the individual records are provided in the supplement. The $\delta^{18}O$ records are given in per mil anomalies with respect to the last 200 years, as is the ATS3 stack.

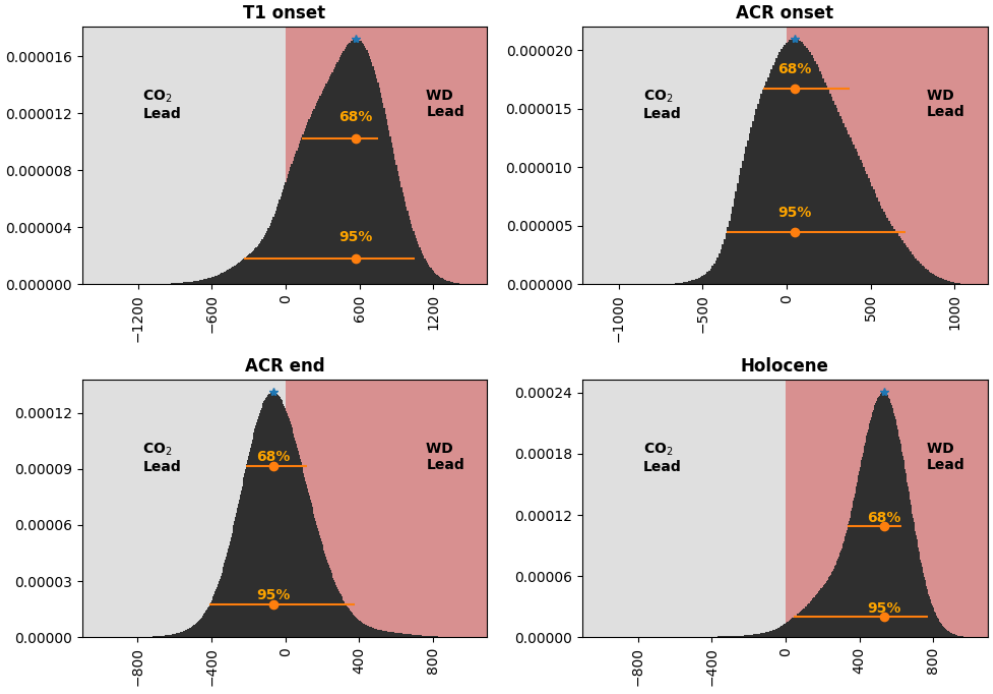

Figure 6. Probability density ρ (y-axis, normalized) of an ATS lead (x-axes, in years) at each of the selected change point intervals (noted on subfigures). Negative x-axis values indicate a CO_2 lead. In the text in each box, the name of the period, the time period in which the lead is calculated, the mean and standard deviation of the lead/lag density (μ and 1σ), and the leading variable are given.

	95 % (lower)	68 % (lower)	Maximum	68 % (upper)	95 % (upper)	Parrenin et al. (2013)	σ
T1 Onset	-338	127	570	751	1045	-10	160
ACR Onset*	-357	-137	50	376	708	260	130
ACR End	-410	-211	-65	117	375	-60	120
T1 End	45	337	532	629	773	500	90

Table 1. Maximum probabilities and central probability intervals for leads and lags at each of the selected change point intervals. Negative x-axis values indicate a CO_2 lead. *The phasing at the ACR onset is sensitive to whether 7 or 8 points are used. Timings with 7 ~~and 8~~ point fits, and for the individual isotopic records, are made available in the Supplementary Materials.

number of points used to make the calculation: with 7 points, we calculate a 240 year lead of ATS3, and with 8 points, we calculate a 50 year lead. In neither of these cases can we exclude synchrony within 95 % probability, and with 8 points, it is well within 68 %. At the ACR end, CO_2 led ATS3, by 65 $\pm$ years within a ~~221~~% range of 228 years to -117 years (a temperature lead) and so again, the possibility of synchrony cannot be excluded within 68 % probability.

At the T1 end, a CO_2 lag is certain. Calculating the phasing between 12.0 ka and 11.0 ka, we obtain an ATS3 lead of 532 years, with a 68% probability range of 337 to 629 years.

3.4 Discussion

Our results refine and complicate the timings and leads and lags identified by the most recent comparable studies (Parrenin et al., 2013; Pedro et al., 2012). We identify a CO_2 change point not treated in these studies at 16 ka, and one before the ACR onset, associated with the centennial-scale rapid rises identified by Marcott et al. (2014). We also treat regional isotopic records, and identify a change point occuring at 13.9 ka in three of the records. None of these change points have a marked counterpart in the other series.

During the major, multi-millenial scale changes which occur at T1 onset and T1 end, Antarctic temperature likely led CO_2 by several centuries. However, during the complex, centennial-scale change at the ACR onset, we cannot calculate a clear lead of either ATS or CO_2, and at the end of the ACR, CO_2 leads temperature. Further, we do not identify a temperature analog for the CO_2 change at 16ka, or an analog in CO_2 of the temperature stabilization in ATS3 after the ACR onset, itself not present in all of the regional $\delta^{18}O$ records, indicating at least some degree of decoupling during these changes. Additionally, the CO_2 changes at the ACR onset and T1 end are overlayed with centennial-scale substructures. Finally, synchrony is within the 2σ uncertainty range for each of the phasings, with the exception of the T1 end.

The changes in CO_2 occurring at the ACR onset, ACR end and the T1 end have been identified to correspond with changes in CH_4 (Marcott et al., 2014), which are thought to originate in tropical wetland sources (Chappellaz et al., 1997; Fischer et al., 2008; Petrenko et al., 2009) and are indicative of Northern Hemisphere and low-latitude temperature changes during the deglaciation (Shakun et al., 2012). Indeed, the CO_2 modes appear to demarcate the rapid changes in the WD CH_4 record, shown in Figure 7.

The beginning of a gradual rise in CH_4 at around 18 ka appears to be near-synchronous with the T1 onset rise in Antarctic temperature. This rise is not seen in Greenland paleotemperature records, where it may have been masked by AMOC-driven wintertime cooling (Buizert et al., 2017) but it appears as well in proxy temperature stacks spanning both the Northern and Southern 0° to 30° latitude bands (Shakun et al., 2012).

Tephras from Mt. Takahe, a stratovolcano located in West Antarctica, have been detected in Antarctic ice cores during a 192 year interval around 17.7 ka. It has been postulated that this eruption may have provoked changes to large-scale SH circulation via ozone depletion, possibly triggering the transition between the gradual SH temperature rise beginning well before 18 ka and the more rapid rise marking the deglaciation (McConnell et al., 2017). The CO_2 mode we find at the deglaciation is coeval with this event within the range of dating uncertainty (Figure 7), and CH_4 visually appears to accelerate concurrently. However, the cumulative probability of the ATS3 change point is much greater before 17.7 ka than after (approximately 80% of the probability density occurs before, see Figure 7); hence our results do not support McConnell et al. (2017)'s proposed volcanic forcing of the temperature change.

Though the T1 onset and the ACR end are both thought to originate in AMOC reductions (Marcott et al., 2014), our results allow for the CO_2-ATS3 phasing to be different during the two events, with the maximum probabilities reversed in

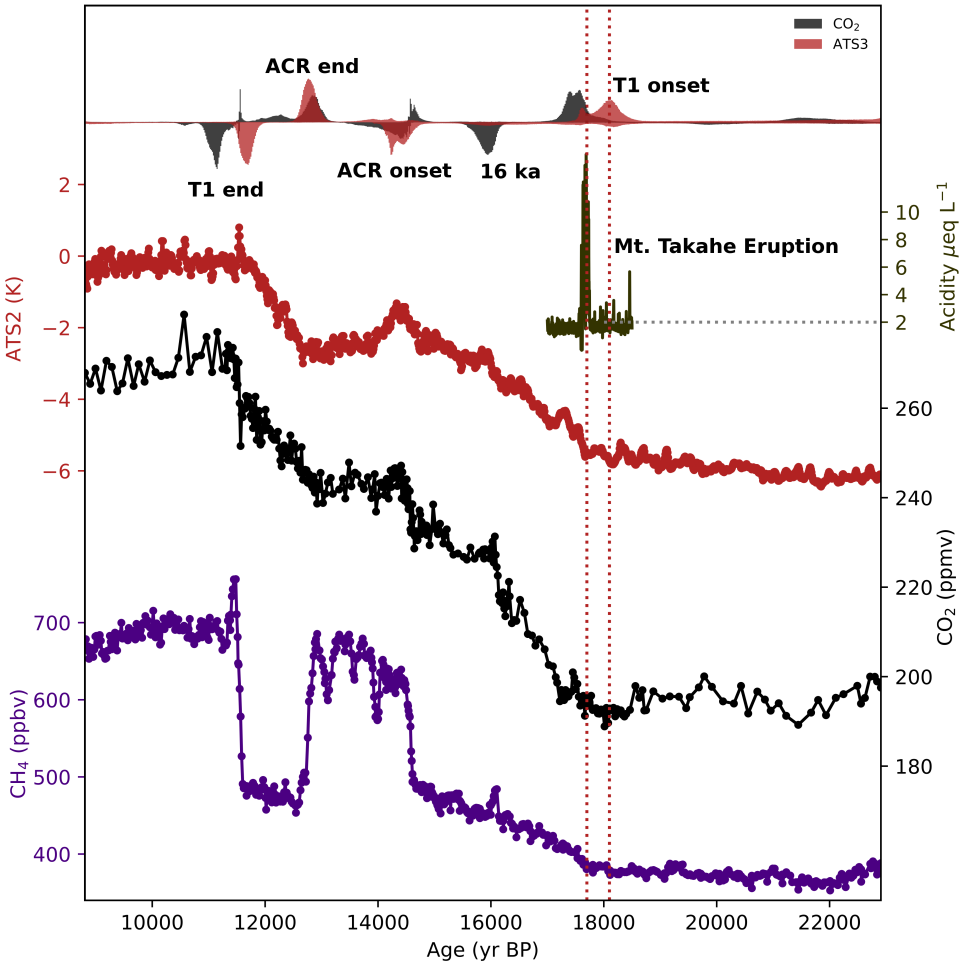

Figure 7. WD CO_2 and ATS3 change point histograms plotted with WD Acidity, ATS3, WD CO_2 and WD CH_4 series (top to bottom). Vertical lines are plotted to highlight select change point modes for the CO_2 (black) and ATS3 (red) series. CH_4 tracks changes in Northern Hemisphere climate. CO_2 modes correspond with rapid changes in CH_4 at the ACR end, ACR onset, 16 ka rise, and the rapid rise preceding the T1 end.

directionality (i.e. with temperature leading at T1 and CO_2 leading at the ACR end, though zero phasing is within 95% error). Though CH_4 appears to change alongside CO_2 during both intervals, the phasings between CO_2 and ATS3 are opposite in direction and different in slope. This hints at a complex coupling, depending on conditions defined by multiple other variables and mechanisms, between CO_2 and Antarctic Temperature. Bauska et al. (2016), for example, hypothesize that an earlier rise of CO_2 at 12.9 ka, driven by land carbon loss or SH westerly winds, might have been superimposed on the millenial-scale trend.

The apparent decoupling between CO_2 and ATS3 at 16 ka also merits further discussion. We do not detect a significant change-point for any of the isotopic records at 16 ka, but the EDML record contains extremely broad uncertainty associated with the significant ACR onset peak, stretching to 16 ka, which indicates that this portion of the EDML time series is indeed notably different in shape from the other records, even if a clear signal is not identified at 16 ka by our method. EDML indeed appears to record changes in AMOC differently than the other isotopic records (Landais et al., 2018; Buizert et al., 2018). CO_2 and ATS3 are similarly apparently decoupled at the temperature change point centered at 14 ka, and this point could be indicative of variability specific to the Pacific/Eastern Indian Ocean sectors, as it is present only in the TALOS Dome and EDC records, and slightly later, around 13.7 ka, in the WAIS Divide record, indicating a cooling trend after the ACR onset which is not clear in the DF or EDML series.

Within the range of uncertainty, the mean of our lead-lag estimates is consistent with the boundaries proposed by Pedro et al. (2012). Our results are consistent with those of Parrenin et al. (2013) for three out of the four change points addressed, but differ considerably at the T1 onset.

The considerable difference between at T1 ~~our result~~ and that of Parrenin et al. (2013) is most likely due to the much higher resolution of the WD CO_2 time series. It is also possible that the result of Parrenin et al. (2013) was limited to a local probability maximum of this change point in the CO_2 series. The addition of the WD paleotemperature record and removal of the Vostok record from ATS3, the updated atmospheric CO_2 dataset, and our more generalized methodology are all, in part, responsible for the differences in computed time delays (SI). This testifies to the importance of data resolution, methodological development, and chronological accuracy in the determination of leads and lags.

4 Conclusions

Our study is a follow-up of the studies by Pedro et al. (2012) and Parrenin et al. (2013) on the leads and lags between atmospheric CO_2 and Antarctic temperature during the last deglacial warming. We refine the results of these studies by using the high resolution CO_2 record from WD; using Δage computed on WD; using a new Antarctic Temperature Stack composed of 5 volcanically synchronized ice core isotope records, developed by Buizert et al. (2018); and using a more precise and complete probabilistic estimate to determine change points. Our methodology detects four major common break points in both time series. The phasing between CO_2 and Antarctic climate is small but variable, with phasing ranging from a centennial-scale CO_2 lead, to synchrony, to a multi-centennial-scale lead of Antarctic climate. This variability of phasings indicates that the mechanisms of coupling are complex. We propose three possibilities: I) the mechanisms by which CO_2 and Antarctic Temperature

were coupled were consistent throught the deglaciation, but can be modulated by external forcings or background conditions that impact heat transfer and oceanic circulation (and hence CO_2 release); II) these mechanisms can be modulated by internal feedbacks that change the response timings of the two series; and/or III) multiple, distinct mechanisms might have provoked similar responses in both series, but with accordingly different lags.

We also explore the hypothesis of regional differences in temperature change in Antarctica. Though the use of individual isotopic temperature records is complicated by influences other than regional temperature, including localized variations in source temperature and ice sheet elevation change we confirm that the deglacial temperature rise did not occur homogeneously accross the Antarctic continent, with significant differences existing between the WAIS Divide and East Antarctic records at the onset of the termination, and smaller potential differences occuring between the East Antarctic records, including a considerably later end of the deglacial warming in the Dome Fuji record.

Hypotheses of relationships between these events should now be reinvestigated with modeling studies. The relationship between CO_2 and Antarctic temperature on longer timescales and during other periods of rapid climate change is also of interest. Additional high-resolution West Antarctic paleotemperature records would allow for a robust investigation of regional differences between West and East Antarctica, and our analysis at the T1 end could be improved with continued high-resolution CO_2 measurements through the beginning of the Holocene. Finally, the continued measurement of high-resolution ice core CO_2 records is essential to understand the relationship between CO_2 and global and regional temperature during the last 800,000 years~~role of CO_2~~.

Code and data availability.

Acknowledgements. We thank Michael Sigl, Jinhwa Shin, Emmanuel Witrant and Amaelle Landais for their support and great help discussing this work and Mirko Severi for his EDC data and support with the volcanic synchronisation. This work is supported by the Fondation Ars et Cuttoli, and by the LEFE IceChrono and CO_2Role projects.

Competing interests. The authors declare that no competing interests are present for this study.

References

Anderson, R., Ali, S., Bradtmiller, L., Nielsen, S., Fleisher, M., Anderson, B., and Burckle, L.: Wind-driven upwelling in the Southern Ocean and the deglacial rise in atmospheric CO2, science, 323, 1443–1448, 2009.

Anklin, M., BARNOLA, J.-M., Schwander, J., Stauffer, B., and Raynaud, D.: Processes affecting the CO2 concentrations measured in Greenland ice, Tellus B, 47, 461–470, 1995.

Barnola, J.-M., Pimienta, P., Raynaud, D., and Korotkevich, Y. S.: CO_2-climate relationship as deduced from the Vostok ice core: a re-examination based on new measurements and on a re-evaluation of the air dating, Tellus B, 43, 83–90, 1991.

Bauska, T. K., Baggenstos, D., Brook, E. J., Mix, A. C., Marcott, S. A., Petrenko, V. V., Schaefer, H., Severinghaus, J. P., and Lee, J. E.: Carbon isotopes characterize rapid changes in atmospheric carbon dioxide during the last deglaciation, Proceedings of the National Academy of Sciences, 113, 3465–3470, 2016.

Berger, A.: Long-term variations of daily insolation and Quaternary climatic changes, Journal of the atmospheric sciences, 35, 2362–2367, 1978.

Buizert, C. and Severinghaus, J. P.: Dispersion in deep polar firn driven by synoptic-scale surface pressure variability, The Cryosphere, 10, 2099–2111, 2016.

Buizert, C., Cuffey, K., Severinghaus, J., Baggenstos, D., Fudge, T., Steig, E., Markle, B., Winstrup, M., Rhodes, R., Brook, E., et al.: The WAIS Divide deep ice core WD2014 chronology–Part 1: Methane synchronization (68–31 ka BP) and the gas age–ice age difference, Climate of the Past, 11, 153–173, 2015.

Buizert, C., Keisling, B. A., Box, J. E., He, F., Carlson, A. E., Sinclair, G., and DeConto, R. M.: Greenland-Wide Seasonal Temperatures During the Last Deglaciation, Geophysical Research Letters, pp. n/a–n/a, doi:10.1002/2017GL075601, http://dx.doi.org/10.1002/2017GL075601, 2017GL075601, 2017.

Buizert, C., Sigl, M., Severi, M., Markle, B. R., Wettstein, J. J., McConnell, J. R., Pedro, J. B., Sodemann, H., Goto-Azuma, K., Kawamura, K., et al.: Abrupt ice-age shifts in southern westerly winds and Antarctic climate forced from the north, Nature, 563, 681, 2018.

Burke, A. and Robinson, L. F.: The Southern Ocean's role in carbon exchange during the last deglaciation, Science, 335, 557–561, 2012.

Caillon, N., Severinghaus, J. P., Jouzel, J., Barnola, J.-M., Kang, J., and Lipenkov, V. Y.: Timing of atmospheric CO_2 and Antarctic temperature changes across Termination III, Science, 299, 1728–1731, 2003.

Chang, C. C. and Politis, D. N.: Robust autocorrelation estimation, Journal of Computational and Graphical Statistics, 25, 144–166, 2016.

Chappellaz, J., Blunier, T., Kints, S., Dällenbach, A., Barnola, J.-M., Schwander, J., Raynaud, D., and Stauffer, B.: Changes in the atmospheric CH4 gradient between Greenland and Antarctica during the Holocene, J Geophys Res Atmos, 102, 15 987–15 997, 1997.

Cuffey, K. M., Clow, G. D., Steig, E. J., Buizert, C., Fudge, T., Koutnik, M., Waddington, E. D., Alley, R. B., and Severinghaus, J. P.: Deglacial temperature history of West Antarctica, Proc Natl Acad Sci U S A, 113, 14 249–14 254, 2016.

Fischer, H., Behrens, M., Bock, M., Richter, U., Schmitt, J., Loulergue, L., Chappellaz, J., Spahni, R., Blunier, T., Leuenberger, M., et al.: Changing boreal methane sources and constant biomass burning during the last termination, Nature, 452, 864, 2008.

Foreman-Mackey, D., Hogg, D. W., Lang, D., and Goodman, J.: Emcee: The MCMC Hammer, Publications of the Astronomical Society of the Pacific, 125, 306, doi:10.1086/670067, 2013.

Fujita, S., Parrenin, F., Severi, M., Motoyama, H., and Wolff, E.: Volcanic synchronization of Dome Fuji and Dome C Antarctic deep ice cores over the past 216 kyr, Climate of the Past, 11, 1395, 2015.

Ghosh, S.: Kernel smoothing: Principles, methods and applications, John Wiley & Sons, 2018.

Goodman, J. and Weare, J.: Ensemble samplers with affine invariance, Comm app math comp sci, 5, 65–80, 2010.

Hays, J. D., Imbrie, J., and Shackleton, N. J.: Variations in the Earth's orbit: pacemaker of the ice ages, Science, 194, 1121–1132, 1976.

Johnsen, S., Dansgaard, W., and White, J.: The origin of Arctic precipitation under present and glacial conditions, Tellus B, 41, 452–468, 1989.

Jones, J. M., Gille, S. T., Goosse, H., Abram, N. J., Canziani, P. O., Charman, D. J., Clem, K. R., Crosta, X., De Lavergne, C., Eisenman, I., et al.: Assessing recent trends in high-latitude Southern Hemisphere surface climate, Nature Climate Change, 6, 917, 2016.

Jouzel, J., Masson-Delmotte, V., Cattani, O., Dreyfus, G., Falourd, S., Hoffmann, G., Minster, B., Nouet, J., Barnola, J.-M., Chappellaz, J., et al.: Orbital and millennial Antarctic climate variability over the past 800,000 years, Science, 317, 793–796, 2007.

Kawamura, K., Parrenin, F., Lisiecki, L., Uemura, R., Vimeux, F., Severinghaus, J. P., Hutterli, M. A., Nakazawa, T., Aoki, S., Jouzel, J., et al.: Northern Hemisphere forcing of climatic cycles in Antarctica over the past 360,000 years, Nature, 448, 912–916, 2007.

Lambert, F., Bigler, M., Steffensen, J. P., Hutterli, M., and Fischer, H.: Centennial mineral dust variability in high-resolution ice core data from Dome C, Antarctica, Climate of the Past, 8, 609–623, 2012.

Landais, A., Capron, E., Masson-Delmotte, V., Toucanne, S., Rhodes, R., Popp, T., Vinther, B., Minster, B., and Prié, F.: Ice core evidence for decoupling between midlatitude atmospheric water cycle and Greenland temperature during the last deglaciation, Climate of the Past, 14, 1405–1415, 2018.

Lisiecki, L. and Raymo, M.: A Plio-Pleistocene stack of 57 globally distributed benthic 0126-026180 records, Paleoceanography, 20, 2005.

Lorius, C. and Merlivat, L.: Distribution of mean surface stable isotopes values in East Antarctica; observed changes with depth in coastal area, Tech. rep., CEA Centre d'Etudes Nucleaires de Saclay, 1975.

Loulergue, L., Parrenin, F., Blunier, T., Barnola, J.-M., Spahni, R., Schilt, A., Raisbeck, G., and Chappellaz, J.: New constraints on the gas age-ice age difference along the EPICA ice cores, 0-50 kyr, Climate of the Past, 3, 527–540, 2007.

Lüthi, D., Le Floch, M., Bereiter, B., Blunier, T., Barnola, J.-M., Siegenthaler, U., Raynaud, D., Jouzel, J., Fischer, H., Kawamura, K., et al.: High-resolution carbon dioxide concentration record 650,000–800,000 years before present, Nature, 453, 379–382, 2008.

Marcott, S. A., Bauska, T. K., Buizert, C., Steig, E. J., Rosen, J. L., Cuffey, K. M., Fudge, T., Severinghaus, J. P., Ahn, J., Kalk, M. L., et al.: Centennial-scale changes in the global carbon cycle during the last deglaciation, Nature, 514, 616–619, 2014.

Masson-Delmotte, V., Schulz, M., Abe-Ouchi, A., Beer, J., Ganopolski, A., Gonzaález Rouco, J., Jansen, E., Lambeck, K., Luterbacher, J., Naish, T., Osborn, T., Otto-Bliesner, B., Quinn, T., Ramesh, R., Rojas, M., Shao, X., and Timmermann, A.: Information from Paleoclimate Archives, in: Climate Change 2013: The Physical Science Basis. Contribution of Working Group I to the Fifth Assessment Report of the Intergovernmental Panel on Climate Change, edited by Stocker, T., Qin, D., Plattner, G.-K., Tignor, M., Allen, S., Boschung, J., Nauels, A., Xia, Y., Bex, V., and Midgley, P., book section 5, p. 383–464, Cambridge University Press, Cambridge, United Kingdom and New York, NY, USA, doi:10.1017/CBO9781107415324.013, www.climatechange2013.org, 2013.

McConnell, J. R., Burke, A., Dunbar, N. W., Köhler, P., Thomas, J. L., Arienzo, M. M., Chellman, N. J., Maselli, O. J., Sigl, M., Adkins, J. F., et al.: Synchronous volcanic eruptions and abrupt climate change 17.7 ka plausibly linked by stratospheric ozone depletion, Proc Natl Acad Sci U S A, p. 201705595, 2017.

Monnin, E., Indermühle, A., Dällenbach, A., Flückiger, J., Stauffer, B., Stocker, T. F., Raynaud, D., and Barnola, J.-M.: Atmospheric CO_2 concentrations over the last glacial termination, Science, 291, 112–114, 2001.

Mudelsee, M.: TAUEST: A computer program for estimating persistence in unevenly spaced weather/climate time series, Computers & Geosciences, 28, 69–72, 2002.

NorthGRIP Project Members: High-resolution record of Northern Hemisphere climate extending into the last interglacial period, Nature, 431, 147–151, 2004.

Parrenin, F., Barker, S., Blunier, T., Chappellaz, J., Jouzel, J., Landais, A., Masson-Delmotte, V., Schwander, J., and Veres, D.: On the gas-ice depth difference (Δ depth) along the EPICA Dome C ice core, Climate of the Past, 8, 1239–1255, 2012.

Parrenin, F., Masson-Delmotte, V., Köhler, P., Raynaud, D., Paillard, D., Schwander, J., Barbante, C., Landais, A., Wegner, A., and Jouzel, J.: Synchronous change of atmospheric CO_2 and Antarctic temperature during the last deglacial warming, Science, 339, 1060–1063, 2013.

Parrenin, F., Bazin, L., Capron, E., Landais, A., Lemieux-Dudon, B., and Masson-Delmotte, V.: IceChrono1: a probabilistic model to compute a common and optimal chronology for several ice cores, Geoscientific Model Development, 8, 1473–1492, 2015.

Pedro, J. B., Rasmussen, S. O., and van Ommen, T. D.: Tightened constraints on the time-lag between Antarctic temperature and CO_2 during the last deglaciation, Climate of the Past, 8, 1213–1221, 2012.

Pedro, J. B., Bostock, H. C., Bitz, C. M., He, F., Vandergoes, M. J., Steig, E. J., Chase, B. M., Krause, C. E., Rasmussen, S. O., Markle, B. R., et al.: The spatial extent and dynamics of the Antarctic Cold Reversal, Nature Geoscience, 9, 51, 2016.

Pedro, J. B., Jochum, M., Buizert, C., He, F., Barker, S., and Rasmussen, S. O.: Beyond the bipolar seesaw: Toward a process understanding of interhemispheric coupling, Quaternary Science Reviews, 192, 27–46, 2018.

Petit, J.-R. and Delmonte, B.: A model for large glacial–interglacial climate-induced changes in dust and sea salt concentrations in deep ice cores (central Antarctica): Palaeoclimatic implications and prospects for refining ice core chronologies, Tellus B, 61, 768–790, 2009.

Petrenko, V. V., Smith, A. M., Brook, E. J., Lowe, D., Riedel, K., Brailsford, G., Hua, Q., Schaefer, H., Reeh, N., Weiss, R. F., et al.: 14CH4 measurements in Greenland ice: investigating last glacial termination CH4 sources, Science, 324, 506–508, 2009.

Rae, J., Burke, A., Robinson, L., Adkins, J., Chen, T., Cole, C., Greenop, R., Li, T., Littley, E., Nita, D., et al.: CO_2 storage and release in the deep Southern Ocean on millennial to centennial timescales, Nature, 562, 569, 2018.

Raynaud, D. and Siegenthaler, U.: Role of trace gases: the problem of lead and lag, Global changes in the perspective of the past, pp. 173–188, 1993.

Raynaud, D., Jouzel, J., Barnola, J., Chappellaz, J., Delmas, R., and Lorius, C.: The ice record of greenhouse gases, Science, 259, 926–926, 1993.

Robinson, P.: Estimation of a time series model from unequally spaced data, Stochastic Processes and their Applications, 6, 9–24, 1977.

Schmitt, J., Schneider, R., Elsig, J., Leuenberger, D., Lourantou, A., Chappellaz, J., Köhler, P., Joos, F., Stocker, T. F., Leuenberger, M., et al.: Carbon isotope constraints on the deglacial CO2 rise from ice cores, Science, 336, 711–714, 2012.

Schwarz, G. et al.: Estimating the dimension of a model, The annals of statistics, 6, 461–464, 1978.

Shakun, J. D., Clark, P. U., He, F., Marcott, S. A., Mix, A. C., Liu, Z., Otto-Bliesner, B., Schmittner, A., and Bard, E.: Global warming preceded by increasing carbon dioxide concentrations during the last deglaciation, Nature, 484, 49–54, 2012.

Silverman, B. W.: Density estimation for statistics and data analysis, Chapman and Hall, 1986.

Skinner, L., Fallon, S., Waelbroeck, C., Michel, E., and Barker, S.: Ventilation of the deep Southern Ocean and deglacial CO2 rise, Science, 328, 1147–1151, 2010.

Sowers, T., Bender, M., Raynaud, D., and Korotkevich, Y. S.: δ15N of N2 in air trapped in polar ice: A tracer of gas transport in the firn and a possible constraint on ice age-gas age differences, J Geophys Res Atmos, 97, 15 683–15 697, 1992.

Stocker, T. F. and Johnsen, S. J.: A minimum thermodynamic model for the bipolar seesaw, Paleoceanography, 18, 2003.

Tarantola, A.: Inverse problem theory, SIAM, 2005.

WAIS Divide Project Members: Onset of deglacial warming in West Antarctica driven by local orbital forcing, Nature, 500, 440–444, 2013.

Williams, D., Peck, J., Karabanov, E., Prokopenko, A., Kravchinsky, V., King, J., and Kuzmin, M.: Lake Baikal record of continental climate response to orbital insolation during the past 5 million years, Science, 278, 1114–1117, 1997.

Supplementary information

Chowdhry Beeman, Gest et al.

Supplementary Information (SI)

Details of the stochastic simulation

A schematic of how residuals between the change point representation and the time series are calculated is included in Figure 1.

In order to eliminate the need to specify an initial fit to estimate the autocorrelation matrix, we perform two subsequent optimizations. During the initialization, we use very rough estimates of the autocorrelation matrix of the residuals and the modeling uncertainty: identity and the standard deviation of the observations, respectively. An automated first guess is proposed by randomly generating the n x_i values and interpolating the y_i values from the observations. This quickly orients the optimization toward the correct region. The optimization is then allowed to run for an initialization period of 25,000 iterations, with 50 individual walkers.

The best fit encountered in the initialization is used to start the true optimization (250,000 iterations with 50 walkers): modeling uncertainty is reestimated as the mean of the absolute residuals on the best fit; and the autocorrelation matrix is reestimated by taking the autocorrelation of the residuals of the best fit. A histogram of the proposals accepted by the second optimization is taken as the final result.

The constant a in equation 3 is set to 2, following Foreman-Mackey et al. (2013).

To conserve computational time, the individual temperature series are run with 10,000 initialization iterations and 100,000 optimization iterations, and the Savitsky-Golay filtered series with 1000 initialization iterations and 50,000 optimization iterations. Tests show that runs with 10,000 optimization iterations achieve reasonable convergence.

Parallel MCMC methodology

To propose updates to the walkers, we apply what Goodman and Weare (2010) refer to as a "stretch move". Consider the ensemble of walkers, in this case representing potential piecewise linear fits $\mathbf{X}$ and an individual walker $\boldsymbol{X}_k^j$ in the ensemble at proposal step j. We select another walker $\boldsymbol{X}_h^j$ from the complementary ensemble $\mathbf{X}_{[k]}^j$, composed of all of the other walkers. Then, a proposal is made to update $\boldsymbol{X}_k$ to W:

$$\boldsymbol{X}_k^j \to W = \boldsymbol{X}_h^j + Z\left(\boldsymbol{X}_k^j - \boldsymbol{X}_h^j\right) \tag{1}$$

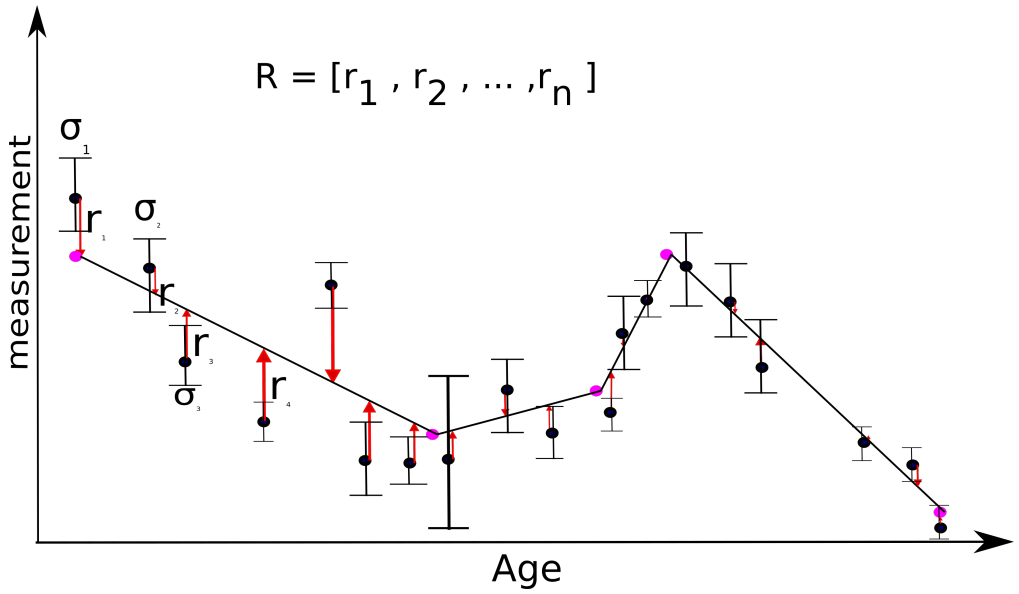

Figure 1. Schematic of the calculation of residuals between a data series and its change point representation. Here, the data series is shown as black points, with 1σ error bars. Change points are shown in pink, and the interpolations between them as black lines. The differences between the data points and the interpolations are shown as red arrows; the residual vector is composed of this distance divided by the uncertainty σ at each point.

GW define the following probability distribution to generate stochastic variable Z:

$$g(Z) \propto \left\{ \frac{1}{Z} \; if \; Z \in \left[\frac{1}{a_Z}, a_Z \right] ; \; 0 \; otherwise \right. \tag{2}$$

where a_Z is a user-defined constant. Proposals are accepted or rejected with acceptance probability

$$P_{\boldsymbol{X}_k^j \rightarrow \boldsymbol{X}_k^{j+1} = W} = \min \left\{ 1, \; Z^{j-1} \frac{exp(-J(W)))}{exp(-J(X_k^j)))} \right\}. \tag{3}$$

BIC and change point sensitivity tests

We calculate the BIC for both series individually, and an additive, normalized BIC to pick the number of change points used. The additive BIC gives 7 as the best number of points to coherently fit both series. Using the individual criteria, 6 points would have been chosen for temperature, and 9 for CO_2, but comparing different numbers of points makes it less clear if the changes reoresented are actually coherent in timescale. These are shown in Figure 2.

We run tests to test the sensitivity of our results to the use of 6,7,8,9 and 10 change points rather than 7 (Figure 3). It is clear from these figures that 5-point fits cannot accurately represent either series; at 6 points, the temperature series begins to be

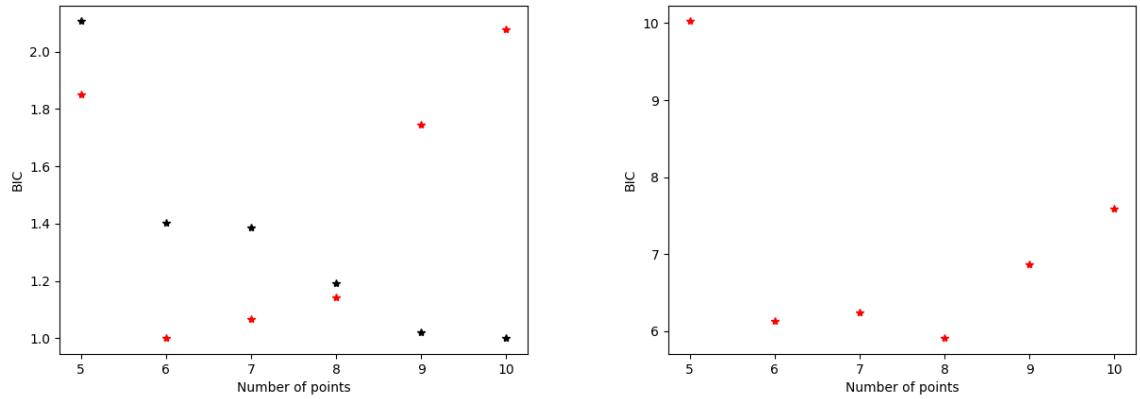

Figure 2. Individual (left, CO_2 in black and ATS3 in red) and cumulative BIC (right) for 5,6,7,8,9 and 10 point (x-axis) runs.

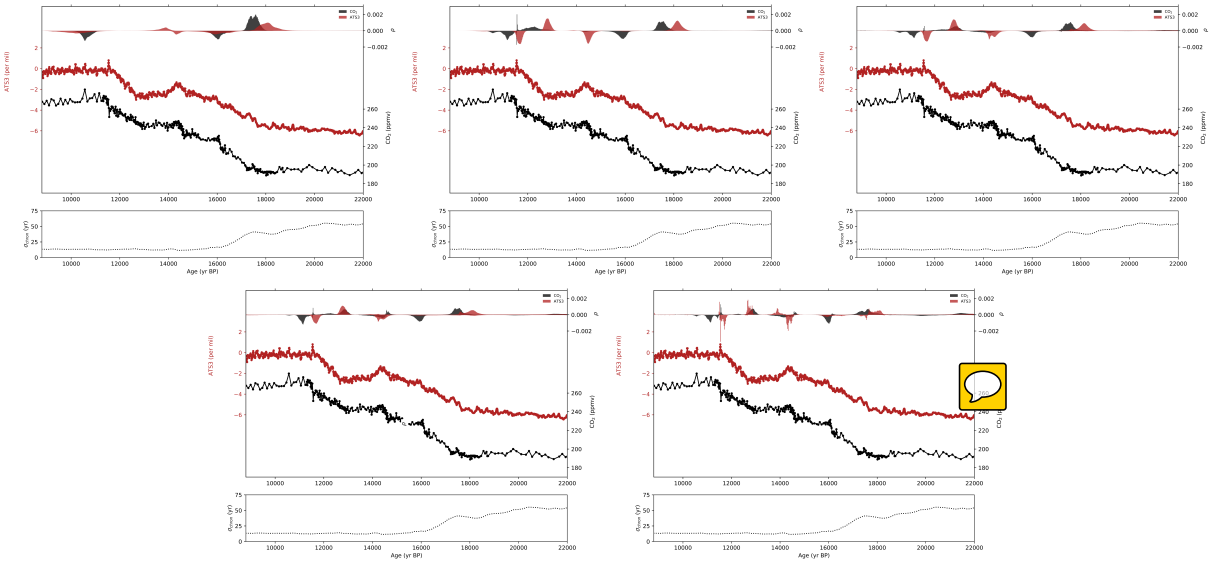

Figure 3. Atmospheric CO_2 (black) and ATS3 histograms of probable change points from the 5,6,7, 8 and 9 (from top left to bottom right) runs of LinearFit.

well-represented, and at 7 points the CO_2 series is appropriately represented. The 7, 8 and 9 point fits do not show significant differences, except at the ACR onset.

Test of AR(1) residuals

We test our AR(1) model by plotting adjacent residuals of the CO_2 series against their predictions, using the robust AR1 model adapted to unevenly spaced time series described in the methods section. The results are shown in figure 4.

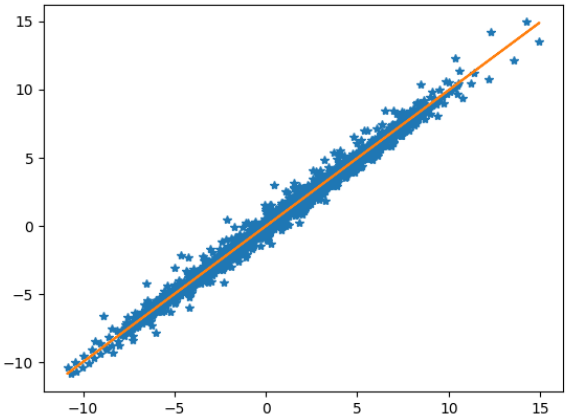

Figure 4. Plot of residuals r_i (x axis) against the predictions made using our AR(1) model $r_i = r_{i-1} \cdot a^{t_i - t_{i-1}}$ (y axis) shown as blue dots, for the CO_2 series after the initialization MCMC procedure. The orange line represents a perfect model fit.

A note on Gaussian Estimates

We avoid providing estimates of change point timings in Gaussian form, i.e. as a mean $\pm$ a standard deviation. This is because the change point histograms we calculate are often skewed, and sometimes even multimodal, with multiple, separate probability peaks in a given time period where change is likely. These peaks can be due to sub-millenial scale variations at these points in the two series.

A test with known lags and covariance

.

We use artificially generated series to test the capacity of our method to fit change points in series with four known change points (plus two end points). For each series, a covariance matrix is used to generate noise with a red component, with a correlation coefficient of 0.8 at 50 years and 0.64 at 100 years away from the central point, and a uniform white component. The noise is scaled to 10% of the standard deviation of the change point values. The results of this test, along with the original change points, are shown in Figure 5.

In Figure 5, note that all of the change points are correctly identified in the histograms, with uncertainties on the order of 100 years. However, a small, but incorrect probability peak is generated around 13 ka. We conclude that gradual changes, such as that around 12 ka, are slightly more difficult to extract from correlated noise even when this noise is modeled, adding some methodological uncertainty which is reflected in the histograms.

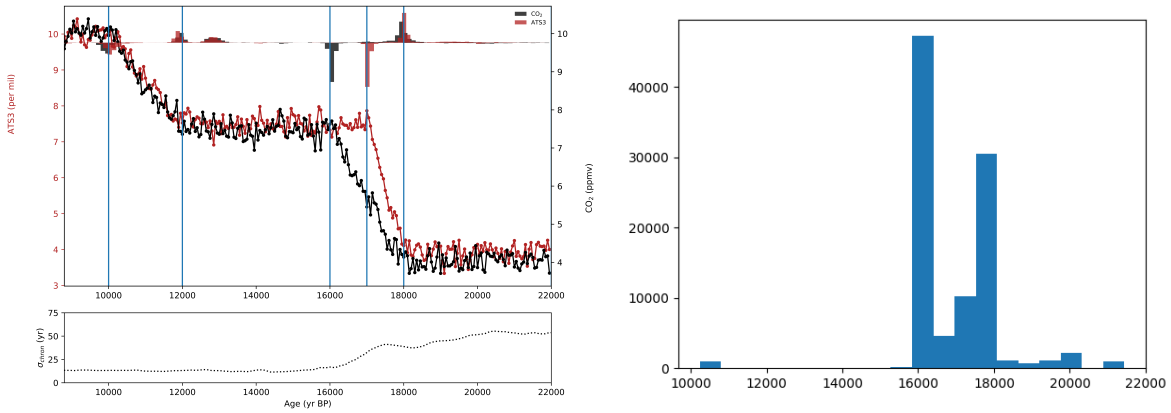

Figure 5. Artificially generated series and generated change point distributions.

References

Foreman-Mackey, D., Hogg, D. W., Lang, D., and Goodman, J.: Emcee: The MCMC Hammer, Publications of the Astronomical Society of the Pacific, 125, 306, doi:10.1086/670067, 2013.

Goodman, J. and Weare, J.: Ensemble samplers with affine invariance, Comm app math comp sci, 5, 65–80, 2010.